frontiers in Earth Science

Pan-arctic trends in terrestrial dissolved organic matter from optical measurements

Paul J. Mann[1*], Robert G. Spencer[2], Peter J. Hernes[3], Johan Six[4], George R. Aiken[5], Suzanne E. Tank[6], James W. McClelland[7], Kenna D. Butler[5], Rachael Y. Dyda[3], Robert M. Holmes[8]

[1]Department of Geography, Northumbria University, United Kingdom, [2]Department of Earth, Ocean and Atmospheric Science, Florida State University, USA, [3]Department of Land, Air, and Water Resources, University of California, USA, [4]Department of Environmental Systems Science, ETH-Zurich, Switzerland, [5]United States Geological Survey, USA, [6]Department of Biological Sciences, University of Alberta, Canada, [7]Marine Science Institute, University of Texas, USA, [8]Woods Hole Research Center, USA

Submitted to Journal:
Frontiers in Earth Science

Specialty Section:
Marine Biogeochemistry

ISSN:
2296-6463

Article type:
Original Research Article

Received on:
05 Oct 2015

Accepted on:
23 Feb 2016

Provisional PDF published on:
23 Feb 2016

Frontiers website link:
www.frontiersin.org

Citation:
Mann PJ, Spencer RG, Hernes PJ, Six J, Aiken GR, Tank SE, Mcclelland JW, Butler KD, Dyda RY and Holmes RM(2016) Pan-arctic trends in terrestrial dissolved organic matter from optical measurements. *Front. Earth Sci.* 4:25. doi:10.3389/feart.2016.00025

Pan-arctic trends in terrestrial dissolved organic matter from optical measurements

Paul J. Mann[1*], Robert G. M. Spencer[2], Peter J. Hernes[3], Johan Six[4], George R. Aiken[5], Suzanne E. Tank[6], James W. McClelland[7], Kenna D. Butler[5], Rachael Y. Dyda[3], Robert M. Holmes[8].

***Correspondence:** Dr Paul J Mann, [1]Department of Geography, Northumbria University, Newcastle-upon-Tyne, UK.
paul.mann@northumbria.ac.uk

Running title: Arctic tDOM export and composition

Keywords: Carbon Cycle, Arctic, Lignin, Colored Dissolved Organic Matter (CDOM), Parallel Factor Analysis (PARAFAC), DOC, Climate Change, Hydrology.

[1]Department of Geography, Northumbria University, Newcastle-upon-Tyne, UK.

[2]Department of Earth, Ocean and Atmospheric Science, Florida State University, Tallahassee, FL, 32306, USA.

[3]Department of Land, Air, and Water Resources, University of California, Davis, California, USA.

[4]Department of Environmental Systems Science, ETH-Zurich, 8092 Zurich, Switzerland.

[5]United States Geological Survey, Boulder, Colorado, USA.

[6]Department of Biological Sciences, University of Alberta, Edmonton, Canada.

[7]University of Texas, Marine Science Institute, 750 Channel View Drive, Port Aransas, TX 78373, USA.

[8]Woods Hole Research Center, Falmouth, MA, 02540, USA.

Abstract

Climate change is causing extensive warming across arctic regions resulting in permafrost degradation, alterations to regional hydrology, and shifting amounts and composition of dissolved organic matter (DOM) transported by streams and rivers. Here, we characterize the DOM composition and optical properties of the six largest arctic rivers draining into the Arctic Ocean to examine the ability of optical measurements to provide meaningful insights into terrigenous carbon export patterns and biogeochemical cycling. The chemical composition of aquatic DOM varied with season, spring months were typified by highest lignin phenol and dissolved organic carbon (DOC) concentrations with greater hydrophobic acid content, and lower proportions of hydrophilic compounds, relative to summer and winter months. Chromophoric DOM (CDOM) spectral slope ($S_{275\text{-}295}$) tracked seasonal shifts in DOM composition across river basins. Fluorescence and parallel factor analysis identified seven components across the six Arctic rivers. The ratios of 'terrestrial humic-like' versus 'marine humic-like' fluorescent components co-varied with lignin monomer ratios over summer and winter months, suggesting fluorescence may provide information on the age and degradation state of riverine DOM. CDOM absorbance (a_{350}) proved a sensitive proxy for lignin phenol concentrations across all six river basins and over the hydrograph, enabling for the first time the development of a single pan-arctic relationship between a_{350} and terrigenous DOC ($R^2 = 0.93$). Combining this lignin proxy with high-resolution monitoring of a_{350}, pan-arctic estimates of annual lignin flux were calculated to range from 156 to 185 Gg, resulting in shorter and more constrained estimates of terrigenous DOM residence times in the Arctic Ocean (spanning 7 months to 2½ years). Furthermore, multiple linear regression models incorporating both absorbance and fluorescence variables proved capable of

explaining much of the variability in lignin composition across rivers and seasons. Our findings suggest that synoptic, high-resolution optical measurements can provide improved understanding of northern high-latitude organic matter cycling and flux, and prove an important technique for capturing future climate-driven changes.

1. Introduction

Northern high-latitude regions contain substantial quantities of organic carbon in perennially and seasonally frozen soils, comprising more than half the entire global carbon soil stock (Tarnocai et al., 2009). Large arctic rivers play an increasingly recognized role in regional carbon cycling by transporting a proportion of this terrigenous material from land to the ocean, whilst also acting as sites for active carbon metabolism and transformation (Holmes et al., 2011; Mann et al., 2015; Spencer et al., 2015; Striegl et al., 2005). Arctic riverine export is substantial enough (~ 10 % of the global freshwater discharge) that it imparts estuarine-like water quality characteristics throughout the Arctic Ocean, influencing coastal salinity structure on a localized basis (Aagaard and Carmack, 1989; McClelland et al., 2011; Serreze et al., 2006). Furthermore, significant quantities of dissolved organic matter (DOM) accompany this freshwater flux causing higher than average dissolved organic carbon (DOC) concentrations in the Arctic Ocean relative to other ocean basins (Hernes and Benner, 2006; Mathis et al., 2005; Opsahl et al., 1999). Six major arctic rivers account for the majority of freshwater flux, each draining vast watersheds on the Eurasian (Kolyma, Ob', Lena, Yenisey) or North American (Mackenzie, Yukon) continents, combined delivering ~ 64 % of the total freshwater supplied to the Arctic Ocean (Holmes et al., 2011).

Arctic rivers are characterized by their strong seasonality and large intra-annual variability in runoff, driven by extreme fluctuations in snow cover and air temperatures. Discharge rapidly peaks with the onset of snow melt and ice-breakup, resulting in dramatic spring freshet events and rapid transport of terrigenous DOM offshore (Amon et al., 2012; Mann et al., 2012; Stedmon et al., 2011a). By contrast, winter months are distinguished by low discharge and DOC concentrations, with

DOM exhibiting lower average aromaticity and molecular weight (O'Donnell et al., 2012; Spencer et al., 2008). Future changes in the fluxes and composition of terrigenous DOM released to and exported from arctic rivers are likely. River discharge across much of the pan-arctic watershed is increasing, particularly during winter months (Déry et al., 2009; McClelland et al., 2006; Peterson, 2002; Rawlins et al., 2010; Smith et al., 2007). Deepening of the seasonally thawed active layer will also result in leaching of deeper soil and permafrost horizons altering the amount and type of DOM liberated to inland waters (Romanovsky et al., 2010). Changes in the quality of DOM affect the reactivity and fate of terrigenous DOM, influencing carbon turnover rates and regional carbon budgets (Holmes et al., 2008; Mann et al., 2012; 2014; Wickland et al., 2012). Tracing future alterations in the composition as well as concentration of riverine DOM is therefore crucial for understanding the effects of climate change.

Lignin phenols are unique biomarkers of vascular plant material and therefore act as sensitive indicators for the terrigenous component of aquatic DOM. As well as providing pertinent information on DOM source, lignin phenols also have the capacity to capture degradative processing and source information (Hernes et al., 2007; Opsahl and Benner, 1995; Spencer et al., 2010a). DOM source and composition have also been assessed via separation of the DOM pool using XAD fractionation techniques. DOC fractionation has been used to differentiate between high molecular weight, aromatic dominated carbon DOM fractions, primarily sourced from allochthonous materials, and those dominated by microbially-derived or photodegraded DOM (e.g. Aiken et al., 1992; Spencer et al., 2012). Despite providing critical information, both lignin phenol and XAD fractionation techniques are costly and extremely time consuming to conduct, limiting their applicability for high-resolution monitoring. The

remote nature of arctic watersheds and the rapid shifts in hydrology make effective sampling and observation of these regions incredibly challenging. Despite far greater understanding of constituent fluxes and biogeochemical cycles across Arctic river systems, much garnered from international sampling campaigns (e.g. PARTNERS, Arctic-GRO; www.arcticgreatrivers.org), insufficient temporal and spatial resolution in measurements still limits our ability to capture changes in terrigenous DOM supply and examine how it may alter under future scenarios. For example, the Arctic Great Rivers Observatory (Arctic-GRO) captures the major seasonal patterns in river chemistry and freshwater discharge across the six major arctic rivers, ensuring identical sampling and analytical protocols, yet is limited with respect to the number of samples that can be feasibly collected. The use of optical measurements, which can be rapidly collected and measured, remotely derived or determined *in-situ,* is one pathway that can help to address these problems.

A number of studies have investigated the ability of optical measurements to capture changes in DOM composition occurring across rivers or over the hydrograph, or to relate optical and lignin-based proxies to improve estimates of terrigenous DOM residence times in the Arctic Ocean (Spencer et al., 2009; Stedmon et al., 2011a; Walker et al., 2013). Recently, chromophoric DOM (CDOM) absorbance measurements from 30 unique US watersheds were shown to correlate to DOM composition, as derived via XAD fractionation, highlighting the potential of optical measurements to improve our understanding of DOM dynamics in fluvial systems (Spencer et al., 2012). Additionally, CDOM absorbance-lignin relationships have been developed for the Yukon River and then scaled to the pan-arctic, assuming similar relative loads of lignin in freshwater fluxes across all arctic rivers (Spencer et al., 2009). Using this approach, Spencer et al., (2009) found that terrigenous DOM

105 export to the Arctic Ocean was higher than previously thought, and thus concluded
106 that a greater proportion must either be modified during transit through estuaries, or
107 removal processes in the Arctic Ocean are greater than previously thought. CDOM
108 fluorescence measurements have also been shown to be potentially useful proxies for
109 lignin phenol concentration and composition in freshwaters (Hernes et al., 2009;
110 Walker et al., 2013). Successful relationships have been reported between CDOM
111 fluorescence, collected as excitation-emission matrices (EEMs) and decomposed
112 using parallel factor analysis (PARAFAC), and lignin measurements across individual
113 arctic rivers, yet pan-arctic relationships remain elusive (Walker et al., 2013). In
114 particular, no studies have attempted to develop relationships between DOM optical
115 properties from across all six arctic rivers and DOC fractionation measurements
116 (XAD), or with vascular plant biomarkers (lignin phenols) as rapid proxies for
117 terrestrial DOC export and composition across the Arctic. Additionally, no studies
118 have examined the utility of combining absorbance and fluorescence techniques to
119 develop arctic proxies for terrigenous DOM export.
120 Here, we characterize the DOM optical properties and composition (XAD and
121 lignin phenol) of the six largest arctic rivers to examine the ability of optical
122 measurements to provide meaningful insights into terrigenous carbon export patterns
123 and biogeochemical cycling across broad spatial scales in the Arctic. Specifically, we
124 attempt to identify common optical indices that trace DOC and lignin phenol
125 concentration and compositional information across all six arctic rivers. Further, we
126 examine the utility of using a combination of absorbance and fluorescence
127 measurements to predict trends in DOC and lignin phenol biomarkers. Finally, we
128 develop, for the first time, a pan-arctic optical proxy for estimating terrestrial OC flux

129 from arctic rivers to the Arctic Ocean and apply our findings to high-resolution
130 optical measurements to improve terrigenous DOC export estimates.
131
132
133 ## 2. Material and Methods
134 ### 2.1 Study Areas and Sample Collection
135 Samples from each of the six largest Arctic rivers (Figure 1) were collected as part of
136 the Arctic Great Rivers Observatory (Arctic-GRO; www.arcticgreatrivers.org). Each
137 of the six rivers was sampled five times per year in 2009 and 2010 (except for 2009
138 on the Yukon with six samples) using a standardized collection method as detailed
139 elsewhere (Holmes et al., 2011; McClelland et al., 2008; Raymond et al., 2007).
140 Depth and width integrated samples were collected from near the mouth of each river
141 (above tidal influence) across the hydrograph, incorporating baseflow, spring melt,
142 and summer conditions. Near-daily surface sampling (0.5 m) was also conducted over
143 the spring freshet hydrographs on each of the six Arctic rivers during both years to
144 provide high-resolution optical measurements for this period (n = 241).
145 Samples collected for DOC concentration, optical properties, and lignin
146 analyses were filtered within a few hours of collection into pre-cleaned high-density
147 polyethylene bottles through pre-rinsed 0.45 µm capsule filters (Geotech or Pall
148 Aquaprep 600) and measured on unfractionated waters. Samples for DOC
149 fractionation were filtered as above and acidified to pH 2.
150
151 ### 2.2 Dissolved Organic Carbon and XAD Fractionation
152 Dissolved organic carbon (DOC) measurements were performed on a Shimadzu
153 (TOC-V) organic carbon analyzer as the mean of 3 – 5 replicate injections where the

coefficient of variance was < 2% (Mann et al., 2012). River water DOC samples were chromatographically separated into operationally defined hydrophobic organic acid (HPOA), hydrophobic neutral (HPON), low molecular weight hydrophilic (HPI), and transphilic organic acid (TPIA) fractions using XAD-8 and XAD-4 resins and established methodologies (Aiken et al., 1992). The amount of organic matter within each fraction is expressed as a percentage of the total DOC concentration and the sample mass of each fraction. The HPOA fraction typically contains more aromatic humic and fulvic acids and the HPI fraction less aromatic and more aliphatic forms of carbon, providing information on DOC composition.

2.3 Lignin Phenol Biomarkers

Lignin phenols were measured via the CuO oxidation method described by Hedges and Ertel, (1982), with modifications as outlined by Spencer et al., (2010b). In brief, filtered whole waters were acidified to pH 2 with 12N HCl, rotary evaporated to ~ 3 mL, and the concentrate transferred to Monel reaction vessels (Prime Focus, Inc.) and dried under vacuum centrifugation. All samples were alkaline oxidized at 155 °C in a stoichiometric excess of CuO, followed by acidification (pH = 1 with 12 N H_2SO_4) and extracted three times with ethyl acetate, passed through Na_2SO_4 drying columns, and taken to dryness under a gentle stream of ultrapure nitrogen. After redissolution in pyridine, lignin phenols were silylated (BSTFA) and quantified on a GC-MS (Agilent 6890 gas chromatograph equipped with an Agilent 5973 mass selective detector and a DB5-MS capillary column; 30 m, 0.25 mm inner diameter, Agilent) using cinnamic acid as an internal standard and a five-point calibration scheme. Eight lignin phenols were quantified for all samples, including three vanillyl phenols (vanillin, acetovanillone, vanillic acid), three syringyl phenols (syringaldehyde, acetosyringone,

179 syringic acid), and two cinnamyl phenols (p-coumaric acid, ferulic acid). One blank
180 was run for every ten-sample oxidations and all samples were blank corrected. Blank
181 concentrations of lignin phenols were low (30 – 40 ng) and consequently never
182 exceeded 5 % of the total lignin phenols in a sample. Lignin phenol concentrations are
183 reported as the sum of the cinnamyl, syringyl and vanillyl phenols ($\sum_8$). Additionally,
184 the carbon normalized sum of the lignin phenols (Λ_8) were calculated.
185
186 **2.4 DOM Absorbance and Fluorescence**
187 UV-visible absorbance was measured in a 1 cm quartz cuvette across 200 – 800 nm at
188 room temperature (20°C) with a dual beam Shimadzu UV-1800 spectrophotometer.
189 Measurements were recorded in triplicate at 1 nm wavelength intervals and referenced
190 against Milli-Q water blanks. Absorbance values were converted to Naperian
191 absorption coefficients by multiplying raw absorbance values by 2.303 and dividing
192 by the pathlength (m) (Hu et al., 2002). The slope (S) of the absorbance spectra was
193 calculated from wavelength ranges spanning 275-295, 290-350, and 350-400 nm and
194 the slope ratio (S_R) determined as $S_{275\text{-}295}/S_{350\text{-}400}$ (Helms et al., 2008). Slope
195 coefficients can provide information pertaining to CDOM composition and source,
196 with steeper values and increasing S_R indicative of lower molecular weight and
197 decreasing DOM aromaticity (Blough and Del Vecchio, 2002; Blough and Green,
198 1995; Helms et al., 2008). Specific UV absorbance ($SUVA_{254}$) was calculated by
199 dividing the decadal UV absorbance at 254 nm by the DOC concentration (Weishaar
200 et al., 2003). The specific UV absorbance ($SUVA_{254}$) has been shown to be positively
201 correlated to percent aromaticity within DOM (Weishaar et al., 2003).
202 Fluorescence was analyzed using a Horiba Fluoromax-4 spectrofluorometer
203 (Jobin-Yvon). Excitation-emission matrices (EEMs) were collected at 20°C in ratio

(S/R) mode over excitation and emission wavelengths of 250 - 450 and 320 - 550 nm, in 5 and 2 nm increments respectively. Measurements were performed with 0.1s integration times and 5 nm slit widths on the excitation and emission monochromators. Instrument specific correction files were applied before further analyses. Fluorescence EEMs were blank corrected from at least daily Milli-Q blanks collected identically to samples. Daily water Raman scans were collected at Ex=350 nm (e.g. Lawaetz and Stedmon, 2009). Raman and Rayleigh-Tyndall scatter were removed and interpolated using the *smootheem* function and absorbance measurements were used to correct EEMs for inner filter effects according to the method of Lakowicz, (2013) within the drEEM toolbox (Murphy et al., 2013). The fluorescence index (FI) was also calculated as the ratio of emission at 470 nm to 520 nm, at an excitation wavelength of 370 nm (Cory et al., 2010; McKnight et al., 2001).

2.5 PARAFAC and statistical analyses

Exploratory analysis of fluorescence EEM data was conducted using parallel factor analysis (PARAFAC) to decompose the number, shape, and amounts of underlying spectral components among samples. PARAFAC was conducted using the drEEM (version 2.0) and *N*-way (version 3.20) toolbox (Murphy et al., 2013) within the MATLAB R2013a environment.

To aid decomposition and provide greater variance within the dataset, additional EEMs (total $n = 645$) collected across a wide range of stream and river environments from the Kolyma River Basin were included and analyzed alongside the Arctic-GRO fluorescence dataset. PARAFAC modeling was performed after normalizing each EEM to its total signal (to unit norm) by dividing by the sum of the squared values of all variables in the sample, and imposing non-negativity constraints,

229 thus negating problems caused by large concentration gradients apparent in seasonal
230 samples (Murphy et al., 2013). The number of components within the model was
231 validated using all of the techniques recommended in Murphy et al., (2013), including
232 examination of systematic variation in the dataset, visualization of spectral loadings,
233 and split half analysis. The final model was successfully validated using four splits of
234 the data and three validation tests across six different dataset halves ($S_4C_6T_3$)
235 (Harshman and Lundy, 1994; Murphy et al., 2013). Fluorescence loadings were
236 calculated after normalizing the dataset ensuring unscaled model scores were
237 recovered.
238 Principle component analysis (PCA; nonrotated solutions) was employed to
239 explore relationships between optical properties, DOC and lignin phenol
240 concentration, and composition using the PLS_Toolbox (Eigenvector, Inc., Seattle,
241 WA v. 8.0) within MATLAB (R2013a). Autoscaling was used on variables measured
242 prior to PCA. Multiple linear regression models were developed using a forward
243 stepwise approach minimizing the Akaike Information Criterion, and were conducted
244 in SPSS v22 (IBM).
245
246 **2.6 Constituent Flux Calculations**
247 Constituent fluxes were estimated using the USGS LoadEstimator software
248 (LOADEST) within the LoadRunner software interface (Booth et al. 2007; Runkel et
249 al., 2004). LOADEST calculates daily constituent flux estimates by generating
250 relationships between measured discharge and element concentrations and was run as
251 in Holmes et al., (2012). Daily discharge data were obtained from US Geological
252 Survey (Yukon), Water Survey of Canada (Mackenzie) and Roshydromet (Kolyma,
253 Lena, Ob' and Yenisey), and are freely available from

http://dx.doi.org/10.5066/F7P55KJN, http://arcticgreatrivers.org/data.html, and the Water Survey of Canada http://wateroffice.ec.gc.ca/mainmenu/historical_data_index_e.html. Corrections were applied to allow for the distance between the discharge measurement station and sample location as has been previously described (Holmes et al., 2012). Any gaps in the discharge data were filled by interpolation, however there were no gaps during peak flow on any river.

3. Results

3.1 Spatial and temporal patterns in chemical fractions of DOC

Total DOC concentrations ranged over the study period from 2.6 to 17.5 mg L^{-1}. Highest average DOC concentrations were measured in the Lena river (15.7 ± 0.9 mg L^{-1}, ± SE) during spring, and lowest during winter in the Yukon river (2.9 mg L^{-1}, n = 1; Table 1). DOC concentrations from all six rivers were correlated with runoff (m^3 km^{-2} d^{-1}; R^2 = 0.44, not shown). Riverine DOC was mainly composed of high contributions from the HPOA fraction, averaging 53 ± 1% across the six Arctic rivers (Table 1). Eurasian rivers contained higher average proportions of the HPOA fraction over the year (54 to 56 ± 2%) relative to the North American Yukon (50 ± 2%) and Mackenzie rivers (45 ± 2%, t-test $p < 0.001$). HPI and TPIA fractions contributed a smaller proportion to bulk DOC, averaging 19 ± 0% and 17 ± 0% respectively. The average HPI and TPIA fractions were less variable than HPOA, ranging from 17 to 23% and 16 to 19% respectively across all sites and seasons (Table 1). HPON fractions generally contributed < 10 % to bulk DOC across rivers and were thus omitted from further study.

278 The composition of DOC was further characterized by calculating specific
279 UV-visible absorbance ($SUVA_{254}$) of DOC and its major chemical fractions (Table 1).
280 Mean $SUVA_{254}$ values of total DOC varied considerably among rivers with lowest
281 values measured in the Mackenzie River (2.5 L mgC^{-1} m^{-1}) and highest in the Yenisey
282 River (3.4 L mgC^{-1} m^{-1}). Mean $SUVA_{254}$ values of the HPOA fraction also varied
283 among rivers with lowest values observed in the Kolyma River (3.6 L mgC^{-1} m^{-1}) and
284 highest in the Yenisey (4.3 L mgC^{-1} m^{-1}), and were consistently higher than bulk DOC
285 highlighting the greater number of highly aromatic compounds represented by this
286 fraction. The $SUVA_{254}$ values of the HPI (1.2 to 2.3 L mgC^{-1} m^{-1}) and TPIA (2.0 to
287 3.1 L mgC^{-1} m^{-1}) fractions were less variable across rivers, and lower than bulk DOC,
288 indicating the presence of a lower relative number of aromatic moieties (Table 1).
289 The contribution of HPOA to the total DOC pool was generally highest during
290 spring months with maximum contributions varying considerably between rivers (47
291 to 60 %; Table 1). Percent contributions of the HPOA fraction were typically lowest
292 during winter flow periods. No clear seasonal differences in the fraction of HPOA
293 present were observed in the Ob' River (55 ± 3 to 57 ±1 %). Mean $SUVA_{254}$ values of
294 total DOC were consistently highest across all rivers during spring months,
295 intermediate during summer months (2.3 to 3.1 L mgC^{-1} m^{-1}), and lowest in winter
296 across all rivers (1.5 to 3.0 L mgC^{-1} m^{-1}; Table 1). $SUVA_{254}$ values of the HPOA
297 fraction followed similar seasonal trends as total DOC. TPIA and HPI $SUVA_{254}$
298 values displayed less clear seasonal patterns (Table 1).
299
300 **3.2 Spatial and temporal patterns in lignin phenols**
301 Mean lignin phenol concentrations ($\sum_8$) varied significantly among the six rivers, with
302 lowest concentrations observed in the Mackenzie River (9.5 μg L^{-1}) and highest in the

303 Lena River (70.0 μg L^{-1}; Table 2). Highest carbon normalized lignin yields (Λ_8) were
304 observed in the Yenisey River, mostly due to lower mean DOC concentrations
305 relative to the Lena River (Table 2). Lowest mean Λ_8 values were measured in the
306 Mackenzie River (0.19 (mg(100 mg OC))$^{-1}$). Lignin values measured in this study
307 were consistent with prior measurements in the Yukon and Russian arctic rivers
308 (Lobbes et al., 2000; Spencer et al., 2009) but notably lower than lignin measurements
309 from the earlier PARTNERS project (Amon et al., 2012).
310 The Lena and Yenisey rivers displayed lowest mean cinnamyl (C) to vanillyl
311 (V) phenol ratios (C/V), indicative of greater contributions of woody versus non-
312 woody sources to bulk DOM of these rivers (Hedges and Mann, 1979). Highest C/V
313 ratios were measured in the Mackenzie and Ob' Rivers (Table 2). Spatial variability in
314 syringyl (S) to vanillyl ratios (S/V) mainly mirrored those of C/V, except for higher
315 S/V values in the Yukon River as compared to the Mackenzie River (Table 2). Higher
316 S/V ratios are indicative of greater proportions of angiosperm versus gymnosperm
317 sources to DOM (Hedges and Mann, 1979).
318 Acid to aldehyde ratios (Ad/Al) have been suggested to provide evidence of
319 the relative degree of DOM degradation, with higher ratios indicating greater
320 degradation of plant tissues (Hedges et al., 1988; Hernes and Benner, 2003; Opsahl
321 and Benner, 1995). Mean ratios of vanillic acid to vanillin (Ad/Al)v ranged from 1.07
322 in the Mackenzie River to 1.48 in the Yukon River (Table 2). Ratios of syringic acid
323 to syringaldehyde (Ad/Al)s varied from 0.84 in the Yenisey to 1.06 in the Mackenzie
324 River.
325 $\sum_8$ values among rivers were strongly linearly related to runoff ($R^2 = 0.69$),
326 suggesting terrigenous DOM export dynamics were largely controlled by hydrology.
327 Accordingly, highest $\sum_8$ concentrations were recorded across all rivers during the

328 spring freshet and lowest concentrations during base flow winter conditions. Highest
329 individual $\sum_8$ values were measured in the Lena River (120 μg L^{-1}) and lowest in the
330 Kolyma and Yukon Rivers (3.8 μg L^{-1}). During the freshet, Λ_8 yields were between
331 2.6 and 4.8 times higher than winter Λ_8 values across sites; the Yenisey River
332 displayed the least variability and the Yukon the greatest (Table 2).
333 C/V and S/V ratios generally declined with increasing runoff across all rivers
334 (Table 2). Acid aldehyde ratios (Al/Ad) were highly variable among rivers, generally
335 increasing with greater runoff, yet in some cases (e.g. Lena River) demonstrated
336 opposing patterns. Highest Ad/Al ratios during the spring freshet may represent the
337 export of greater quantities of largely 'fresh' microbially unprocessed DOM relative
338 to later in the year (Hernes et al., 2007; Spencer et al., 2008; Amon et al., 2012).
339
340 **3.3 Chromophoric and fluorescence DOM of arctic rivers**
341 The absorbance coefficient of CDOM at 350 nm (a_{350}) ranged from 2.3 to 42.6 m^{-1}
342 among rivers and seasons, and similar to DOC and $\sum_8$ concentrations, generally
343 increased with greater freshwater runoff ($R^2 = 0.57$, $p < 0.001$, $n = 60$; Supplemental
344 Table 1). Spectral slope values ($S_{275\text{-}295}$, $S_{290\text{-}350}$, $S_{350\text{-}400}$) steepened with decreasing
345 runoff, in good agreement with previous studies (Spencer et al., 2009; Stedmon et al.,
346 2011a), indicating the export of lower molecular weight material, or DOM with
347 decreasing aromaticity as discharge rates decline (Blough and Del Vecchio, 2002;
348 Blough and Green, 1995). The slope ratio (S_R) showed an opposing pattern to spectral
349 slopes, declining at higher runoff rates thus confirming an increase in DOM molecular
350 weight during the spring freshet and reduction during winter base flow months
351 (Helms et al., 2008; Spencer et al., 2010a; 2012).

352 Fluorescence index (FI) values were similar across rivers and averaged 1.34 ±
353 0.01 across all sites and sampling dates reflecting DOM from a mixture of terrigenous
354 and microbial sources (McKnight et al., 2001; Supplemental Table 1). Highest FI
355 values were measured across all rivers during winter months (mean 1.41 ± 0.03),
356 reflecting a potentially higher contribution of microbial derived or lower aromaticity
357 DOM during this period. Lowest FI values among rivers (mean 1.31 ± 0.01),
358 indicative of greatest terrigenous and aromatic DOM supply, were observed during
359 the high discharge spring freshet.
360
361 **3.4 Parallel factor analysis (PARAFAC)**
362 The PARAFAC analysis of DOM excitation-emission scans collected from all six
363 arctic rivers over the hydrograph identified seven unique components of DOM
364 fluorescence (Fig. 2; Supplemental Fig. 1). The spectra of each component identified
365 were compared with the open fluorescence database (openfluor.org) containing
366 spectra from previous studies (currently 53 studies) detailing PARAFAC models. All
367 seven components closely matched (tucker congruence coefficient, TCC >0.95;
368 Tucker, 1951) the excitation and emission spectra of previously identified
369 components from 37 independent studies (Table 3).
370 Four of the seven AG components were very closely related (TCC ≥ 0.97) to
371 those reported in the five-component Horsens catchment model (Murphy et al., 2014).
372 For each of the seven components identified here, at least three independent studies
373 had previously identified statistically similar spectra, except for component AG3 for
374 which there was only a single match. Table 3 provides information and a description
375 of the seven components identified.

376 AG3 was closely related (TCC = 0.97) to C1 in Murphy et al., (2014) where it
377 was identified as displaying an emission spectrum identical to syringaldehyde, a
378 product of lignin breakdown. The AG model shared two components with a five-
379 component PARAFAC model explaining florescence DOM collected from five of the
380 major Arctic rivers sampled here over 2004-2005 (Walker et al., 2013). AG6 was
381 similar (TCC >0.95) to C1 from this model (Walker et al., 2013), while AG7 was
382 identical to C5, which can be described as tryptophan-like and has been commonly
383 associated with biological production in surface waters (Determann et al., 1994).
384 Two AG model components were also highly related to components
385 previously reported in sea ice. AG1 was comparable to the terrestrially-derived
386 component C2 found within Baltic sea ice (Stedmon et al., 2007). AG1 was also
387 identical to C3 in coastal Canadian Arctic waters, which proved to be highly
388 positively correlated with $\sum_8$ (Walker et al., 2009). AG5 was identical to C6 in a study
389 of Antarctic sea ice brines (Stedmon et al., 2011b), and is similar to the commonly
390 described 'M' peak across a wide range of environments (Coble, 1996; 2007; Fellman
391 et al., 2010).
392 Component AG4 contributed the greatest (23.4% ±0.6%) and AG7 the lowest
393 percentage (5.1% ±0.3%) towards total DOM fluorescence across all rivers and
394 seasons. In contrast to previous studies, no consistent pan-arctic seasonal or spatial
395 patterns were apparent in the fluorescence loadings or percent contribution of any of
396 the seven components (Walker et al., 2009). Individual patterns in fluorescence were,
397 however, observed across rivers and seasons. Component AG1 contributed a
398 substantially higher proportion of total fluorescence during the summer months in the
399 Kolyma (20.5% ± 0.1%) and Lena Rivers (20.6% ± 0.6%) relative to each of the other
400 rivers (16.8 to 17.7%), yet comprised similar amounts during the rest of the year.

401 Similarly, the proportion of AG3 was significantly higher in the Kolyma (23.2% ±
402 0.8%) and Lena (19.1% ± 1.4%) Rivers relative to the others (11.3% to 17.6%) during
403 the summer months alone. Opposing patterns were observed in AG6, with
404 significantly lower proportions in the Kolyma (4.4% ± 0.1%) and Lena Rivers (5.3%
405 ± 0.6%) relative to the others, in particular the Yenisey (9.7% ± 1.2%) and Ob' Rivers
406 (8.4% ± 1.8%). The Mackenzie River contained high proportions of AG7 during the
407 summer months (6.7% ± 1.1%) relative to all other rivers (3.9 to 5.2%).
408
409
410 **4. Discussion**
411
412 **4.1 Optical measurements, DOC concentration and DOM composition**
413 CDOM absorption (a_{350}) correlated strongly with DOC concentration across all rivers
414 during the standard Arctic-GRO sampling over 2009 and 2010 ($R^2 = 0.89$; $p < 0.001$; n
415 = 60, not shown). This strong positive linear relationship persisted when DOC
416 concentration and a_{350} values from the additional high-resolution measurements
417 collected over the freshet period were included ($R^2 = 0.81$; $p < 0.001$; $n = 301$; Figure
418 3a). Despite this robust pan-arctic relationship however, when rivers were analyzed
419 independently significant differences in the slopes and intercepts for the DOC to a_{350}
420 relationships were observed (Table 4). This indicates that the relative amount of non-
421 chromophoric DOM varies across Arctic rivers, and suggests that the proportion of
422 DOC per unit CDOM within individual river basins should in the future be separately
423 determined (Table 4). Interestingly, we also find that the variability in river-specific
424 slope and intercepts were well-explained by total annual river discharge, with
425 increasing discharge resulting in higher DOC:a_{350} intercepts ($R^2 = 0.58$; $p < 0.05$, not

shown) and shallower slopes ($R^2 = 0.72$, $p < 0.05$, not shown). The relationship between annual discharge and DOC:a_{350} intercepts improved significantly ($R^2 = 0.98$; $p < 0.01$) with the exclusion of the Mackenzie River. Thus, greater dilution of DOM and export of non-chromophoric organics occurs with increasing total discharge. The different relationship observed in the Mackenzie may be due to its relatively low DOM yield, high abundance of suspended sediments, as well as high proportion of lakes relative to other watersheds (Stedmon et al. 2011a).

HPOA fraction was closely related to $S_{275\text{-}295}$ across rivers, with the relative proportion of HPOA decreasing with steepening slope ($R^2 = 0.65$; $p < 0.001$, $n = 58$), as previously reported across five of these rivers in 2004-2005 (Walker et al., 2013). This suggests that average DOM molecular weight and aromaticity decreases as the proportion of HPOA declines, in good agreement with a number of previous studies (Neff et al., 2006; O'Donnell et al., 2012; Spencer et al., 2012; Striegl et al., 2007). This was further supported by a positive linear relationship between average HPOA and $SUVA_{254}$ across rivers ($R^2 = 0.56$, $p < 0.01$, Supplemental Fig. 2). The DOM composition of winter flow has been shown to contain lower proportions of the HPOA fraction as compared to HPI, with lower $SUVA_{254}$ values relative to summer and spring months in the Yukon River (O'Donnell et al., 2012). The aromaticity of the HPOA fraction (HPOA-$SUVA_{254}$), was negatively correlated with FI ($R^2 = 0.32$, $p < 0.001$, $n = 47$, not shown), confirming the role of terrigenous supply on delivering increased proportions of aromatic organics to the exported DOM pool.

No pan-arctic relationships were observed between any of the fluorescence component loadings and DOC concentration or composition (Supplemental Tables 2 & 3). However, weak yet significant relationships were observed between the relative proportions of components AG3 and AG4 to total fluorescence and DOC

concentrations across all six rivers (R^2 = 0.15 and 0.16 respectively, $p < 0.01$). AG3 proportions generally decreased with increasing DOC concentrations, where AG4 proportions increased with greater DOC concentrations. These relationships were largely driven by particularly strong relationships across the Kolyma and Lena Rivers (AG3 R^2 = 0.70; AG4 R^2 = 0.70, $p < 0.001$). The relatively weak pan-arctic relationships we observe here contrasts with the findings of Walker et al., (2013), whom report strong correlations between DOC concentration and fluorescence loadings. These conflicting findings may have been due to the additional normalization step we applied to scale each EEM to its total signal, thus ensuring the model focused entirely on compositional rather than concentration gradients. Alternately, the addition of a significant number of EEMs from upstream sources may have resulted in the validation of different components during PARAFAC decomposition. The latter seems unlikely however, as two of the seven components were spectrally identical (TCC >0.95) to the PARAFAC model used by Walker et al., (2013), including component AG6 which was spectrally indistinguishable from a component (C1) identified as most closely tracing DOC and $\sum_8$ concentrations. Other potential causes include differences in the treatment of inner filter effects. We applied a commonly employed post-hoc method by Lackowicz (2013) to correct our EEMs for inner filter effects using parallel CDOM absorbance measurements, whereas Walker et al. (2013) diluted samples prior to measurement. Our method more closely reflects direct measurement of field samples and is similar to information that could be derived from *in-situ* instruments. Our findings suggest that loadings derived from fluorescence EEMs decomposed using PARAFAC may not always be useful when tracing DOC concentration.

476 **4.2 Optical measurements and lignin concentration and composition**

477 CDOM (a_{350}) measurements were highly correlated to $\sum_8$ across all six rivers basins
478 ($R^2 = 0.93$; $p < 0.001$; $n = 31$; Figure 3b). This represents the first pan-arctic
479 relationship to be reported between a_{350} and $\sum_8$ across all six major rivers. The
480 observed linear relationship ($\sum_8 = -8.06 \pm 2.71 + (2.80 \pm 0.14 a_{350})$) was similar to, yet
481 displayed a slightly higher slope, than reported in Spencer et al., (2008) for the Yukon
482 River Basin only ($\sum_8 = -6.67 \pm 2.88 + (2.21 \pm 0.11 a_{350})$. Previous studies have
483 reported a much steeper linear relationship between a_{350} and $\sum_8$, with the Mackenzie
484 and Ob' Rivers grouping separately from the Kolyma, Lena and Yenisey (Walker et
485 al., 2013). The steeper slope of the previously reported relationship is caused by the
486 substantially higher (often greater than double) lignin concentrations ($\sum_8$) reported in
487 Amon et al., (2012) and used in Walker et al., (2013) relative to those presented here.
488 The differences in $\sum_8$ concentrations may be due to methodological differences, as
489 suggested by Walker et al., (2013), and raises concern over future potential in
490 comparing datasets. For example, comparison of data from Spencer et al., (2008) in
491 Walker et al., (2013) suggested low relative lignin concentrations in DOM from the
492 Yukon, whereas we identify a similar $\sum_8$ to a_{350} relationship across all six major arctic
493 rivers.

494 Carbon normalized lignin (Λ_8) yields decreased exponentially with steepening $S_{275\text{-}295}$
495 values across all rivers and seasons ($R^2 = 0.80$; $p < 0.01$, $n = 31$; Table 2 and
496 Supplementary Table 1). Steepening $S_{275\text{-}295}$ values were associated with decreasing
497 runoff rates (section 3.3), thus Λ_8 yields typically increased as DOM average
498 molecular weight and aromaticity increased, and during spring and summer months in
499 response to greater allochthonous DOM supply.

500 Lignin phenols have been shown to comprise a major component of the HPOA
501 fraction (Spencer et al., 2008; 2010a; Templier et al., 2005). This was confirmed by a
502 significant positive correlation between proportion HPOA and Λ_8 yields ($R^2 = 0.71$, p
503 < 0.001, $n = 29$; not shown). Lignin phenol biomarkers thus appear capable of
504 providing information on the biogeochemical cycling of the entire hydrophobic DOM
505 pool, which comprises up to two-thirds of aquatic DOM.
506 Lignin phenol C/V ratios increased with steepening $S_{275\text{-}295}$ values ($R^2 = 0.54$;
507 $p < 0.001$, $n = 31$) and declining total $SUVA_{254}$ values ($R^2 = 0.48$; $p < 0.001$, $n = 31$)
508 (Tables 1 and 2 and Supplementary Table 1). The overall decline in C/V ratios with
509 increasing freshwater runoff appears to represent increased contributions of lignin
510 from litter and surface soil layers alongside greater proportions of aromatic and higher
511 molecular weight DOM export (Hedges and Mann, 1979). These findings however
512 appear counterintuitive relative to what we currently understand about hydrologic
513 flow paths and sources of DOM to aquatic systems. Non-woody litter tissues
514 associated with surficial, predominantly overland flow paths are expected to impart
515 higher C/V ratios and lower degradative alteration than observed in DOM exported
516 during base flow conditions derived from deeper flow paths. Physical processes, such
517 as leaching and sorption, can also influence lignin phenol ratios (Hernes et al., 2007;
518 2008) and may therefore be responsible for the observed trends. S/V and acid to
519 aldehyde ratios did not correlate closely with spectral slope, $SUVA_{254}$, or S_R values.
520 The overall trends in lignin phenol composition we report are similar to those
521 previously shown across Arctic rivers (Amon et al., 2012; Spencer et al., 2008; 2009),
522 and demonstrate a shift from predominantly modern surface-derived and lignin-rich
523 DOM during the spring freshet to older, less lignin-rich DOM under base-flow winter
524 conditions.

525 No pan-arctic relationships were observed between fluorescent PARAFAC
526 component loadings and lignin phenol concentration or composition measures
527 (Supplemental Tables 2 & 3). A weak yet significant relationship was however found
528 between the relative proportions of components AG3 and AG4 to $\sum_8$ concentration
529 ($R^2 = 0.18$; $p < 0.02$) but again was significantly stronger across the Kolyma and Lena
530 Rivers in particular ($R^2 = 0.79$; $p < 0.001$). FI values positively correlated with
531 increasing C/V ratios ($R^2 = 0.48$, $p < 0.001$, $n = 30$) confirming losses in the
532 proportion of woody tissues with increased autochthonous or less aromatic DOM
533 supply.
534
535 **4.3 Linking optical properties to Arctic river DOM composition**
536 Underlying patterns and relationships between optical DOM parameters, DOC, and
537 lignin were further explored using principle component analysis (PCA), which can
538 identify the structure of data that best explains the variance within the dataset. The
539 optical properties of DOM varied with season across all rivers, as demonstrated by
540 PCA plots containing PARAFAC fluorescence components (percent contribution) and
541 spectral slope information. The addition of FI and S_R values added little additional
542 information to the PCA analyses. Furthermore, $SUVA_{254}$ followed identical patterns
543 to each of the spectral slope parameters and its inclusion led to similar PCA plots.
544 These indices were therefore omitted from the final PCA model for clarity. Three
545 principle components (PCs; eigenvalue > 1) were identified that together explained
546 80% of the total variance in the optical data (PCopt 1-3). PC1opt was related to
547 increasing fluorescence contributions from AG3, AG1, and AG5, but decreasing
548 contributions from AG6, AG4, and AG2 (Fig. 4). Components AG1, 3, and 5
549 represent DOM fluorescence signatures that have all previously been reported to be

susceptible to microbial processing, or to be a byproduct of vascular material degradation (Table 3 and references herein). These fluorescence signatures may therefore represent indicators of 'degraded' or processed humic-like components. In contrast, components AG 2, 4, and 6 appear to represent more unreactive and stable components, previously being described as refractory in nature and shown not to co-vary with bacterial production (Table 3). PC1opt may therefore reflect potential reactivity or be an indicator of prior DOM processing. PC2opt appeared to be related to the shifting molecular weight of DOM, as indicated by strong relationships with changes in all spectral slopes (and $SUVA_{254}$, not shown), whereas PC3opt was positively related to increased protein-like or phenolic DOM (AG7) and decreasing contributions from humic-like DOM (AG2 and AG1). PCA models run with only PARAFAC components contained two principle components, each indistinguishable from PC1opt and PC3opt, demonstrating that information on DOM potential reactivity and the relative contribution of protein-like versus humic-like could be obtained from fluorescence measurements alone.

Seasonal changes in DOM composition across all six rivers were most clearly separated along the PC2opt axis, with spring waters containing higher molecular weight material with shallower spectral slopes than summer and winter month waters. Positive scores on PC3opt during spring and winter months, relative to summer, suggest greater contributions of protein-like or phenolic material (as inferred by the proportion of component AG7), potentially representing reductions in allochthonous supply or increased export of fresh organics from surface layers, respectively. No clear separation among the six different rivers was apparent with optical properties alone across any of the PC axes.

574 To examine if the observed trends in DOM optical properties were related to
575 geochemical changes in organic matter we conducted a separate PCA incorporating
576 all lignin phenol and DOC fractionation variables. We subsequently compared the
577 identified PCs with those extracted from optical measurements alone. Two PCs
578 (PCmol 1-2) were identified, in combination explaining 67 % of the total variance in
579 geochemical composition (Fig. 5). PC1mol positively related to increasing HPOA, $\sum_8$,
580 and Λ_8 contributions and negatively with C/V ratio and proportions of the
581 hydrophobic neutral and hydrophilic fractions. The axis therefore primarily separates
582 seasonal variability observed in DOC, with spring months delivering greater
583 proportions of HPOA with high concentrations of $\sum_8$ and Λ_8 values. PC2mol most
584 strongly correlated to (Ad/Al) ratios suggesting it represented changing proportions of
585 DOM degradation state. S/V ratio was also positively related with PC2mol, indicating
586 that shifts in the relative proportions of sources waters may also be represented by this
587 axis or similar processes (e.g. leaching and sorption) may be driving the observed S/V
588 and (Ad/Al) ratios.

589 Comparing separate PCs from both optical and geochemical PCAs across all
590 sites and sampling dates, only a single significant positive correlation was observed
591 between PC2opt extracted from optical characteristics and PC1mol from DOC and
592 lignin composition (r^2 = 0.65, p < 0.001, n = 30; Fig. 5). Thus, seasonal variability in
593 DOC composition was explained by relatively simple CDOM slope (and $SUVA_{254}$)
594 metrics. Separating over seasons, PC1opt correlated significantly with PC2mol during
595 the summer (r^2 = 0.85, p < 0.05, n = 8) and winter months (r^2 = 0.65, p = 0.06, n = 6),
596 but not over spring periods across all six rivers. This further suggests that shifts in the
597 relative proportions of PARAFAC components reflect shifts in the relative
598 degradation signature of DOC inferred from acid:aldehyde ratios during certain

599 periods of the year. Information pertaining to the source (S/V ratios) of DOM may
600 therefore also be contained in the relative ratio of more or less reactive or degraded
601 PARAFAC components. Interestingly, (Ad/Al)v ratios have also been shown to
602 correlate with the average ^{14}C age of DOC within these Arctic rivers (Amon et al.,
603 2012). Fluorescence measurements may therefore provide information pertaining to
604 both the age and degradation history of DOM across Arctic systems. Broad patterns in
605 the temporal variability of DOM composition over pan-arctic scales therefore appear
606 best captured using simple CDOM spectral slope and $SUVA_{254}$ measurements.
607 Information on DOM processing, source, and age may instead be contained within
608 CDOM fluorescence spectra and the relative contributions of PARAFAC components.
609

610 **4.4 Modeling terrestrial biomarkers with optical measurements**

611 We ran a series of multiple linear regression models with the aim of predicting Λ_8,
612 C/V, S/V, (Ad/Al)s, and (Ad/Al)v across all sampling dates and rivers. Incorporating
613 absorbance (a_{350}, slope ratios, $SUVA_{254}$,) and fluorescence optical measurements (FI,
614 % PARAFAC component contributions) as potential parameters, Λ_8 ($R^2 = 0.76$; Fig. 6
615 a), C/V ($R^2 = 0.70$; Fig. 6 b) and S/V values ($R^2 = 0.68$, Fig. 6 c) could be
616 successfully predicted by model fits (all $p < 0.001$; n=31). Modeled values for
617 (Ad/Al)v were also strongly correlated with observed values ($p < 0.001$), but
618 predictive capability was low ($R^2 = 0.49$, not shown). Model fits failed to accurately
619 predict the variability in the (Ad/Al)s ratios ($p > 0.05$).

620 The optical parameters providing the greatest predictive power varied between
621 each lignin parameter. Models predicting Λ_8 only incorporated $S_{275\text{-}295}$ and a_{350} values
622 ($\Lambda_8 = 1.136 \pm 0.250 + (55.742 \pm 14.152 * S_{275\text{-}295}) + (0.006 \pm 0.003 * a_{350})$). Modeling
623 C/V values also used $S_{275\text{-}295}$ and a_{350} values (alone explaining 58% of the variance),

but improved with inclusion of %AG7 and $S_{290\text{-}350}$ values (C/V = -0.153 ±0.127-(57.265 ±17.921*$S_{275\text{-}295}$)+(0.040 ±0.015*%AG7)+(45.225 ±18.604*$S_{290\text{-}350}$)-(0.002*a_{350})). Models explaining S/V values incorporated $S_{290\text{-}350}$, a_{350}, %AG7, and FI (S/V = -2.704 ±0.827+(64.131 ±14.843*$S_{290\text{-}350}$)+(2.896 ±0.695*FI)-(0.009 ±0.002*a_{350})+(0.074 ±0.027*%AG7)). S/V could not be explained with absorbance measurements alone. The ability to predict lignin composition as well as concentration using fluorescence measurements has previously been reported using partial least squares models of samples collected over a two year period on the Sacremento River/ San Joaquin River Delta, California (Hernes et al., 2009). The authors demonstrated that the most significant predictive capability for lignin was within the commonly referred to protein-like fluorescence region (similar to our component AG7). Fluorescence of propylphenol monomers, that structurally comprise lignin, can generate fluorescence signatures in a similar region to amino acids and in the region known as 'protein-like', thus our results may indicate information obtained from changes in phenolics rather than amino acid or proteins (Hernes et al., 2009). Therefore, it seems that rapid, inexpensive optical measurements may be capable of acting as a proxy for dissolved lignin compositional parameters as well as concentration across pan-arctic scales and catchments. The combination of absorbance and fluorescence metrics can also add predictive power when attempting to predict shifts in the composition of terrigenous DOC.

4.4 Improving terrigenous OC export estimates

The absorbance coefficient at 350nm (a_{350}) has previously been shown to be a sensitive and inexpensive proxy for lignin phenol concentration across a range of freshwater environments within Arctic river basins (Spencer et al., 2008; 2009;

649 Stedmon et al., 2011a). Furthermore, increased sampling frequency of Arctic rivers
650 has led to significantly higher and better constrained DOC export estimates,
651 particularly after the inclusion of samples from across the spring freshet period (e.g.
652 Köhler et al., 2003; Striegl et al., 2005; Holmes et al., 2012). Here, we investigate if
653 the combination of a lignin proxy with high-resolution monitoring of a_{350} over Arctic
654 river hydrographs may be used to develop improved estimates of pan-arctic
655 terrigenous DOC export, hereby refining land-to-ocean carbon flux estimates.

656 CDOM-derived lignin phenol concentrations ($lignin_{350}$) were calculated using
657 the linear regression of $\sum_8$ and a_{350} (Fig. 3b). $Lignin_{350}$ values were derived from a_{350}
658 measurements taken from waters collected over the main Arctic-GRO sampling
659 campaign and additional high-resolution samples taken over the freshet hydrographs.
660 Inclusion of near-daily absorbance measurements collected over the peak discharge
661 period alongside measurements spanning the entire year was crucial in adequately
662 constraining fluxes during the spring freshet, when the majority of annual lignin
663 export is expected (Amon et al., 2012; Spencer et al., 2008). $Lignin_{350}$ concentrations
664 calculated for samples with concurrent $\sum_8$ measurements were highly correlated across
665 all Arctic rivers (r^2 = 0.92, p < 0.01, n = 31, Standard error of estimate, SE_E = 8.8%)
666 demonstrating the robust nature of this approach.

667 Daily model loads (mass d^{-1}) of $\sum_8$ in each river were calculated using a
668 hydrologic load estimation model (LOADEST) integrating the $lignin_{350}$
669 concentrations and twelve years of daily discharge data ranging from 1999 – 2010
670 (see Methods). Estimated lignin loads varied from 4.0 Gg y^{-1} in the Mackenzie to 43.1
671 Gg y^{-1} in the Lena River (Table 5). The Lena, Yenisey, and Ob' Rivers export > 85 %
672 of the total annual lignin discharge from the six largest Arctic rivers, a proportion that
673 is very similar to that found by Amon et al., (2012). Flux estimates using lignin

674 phenol concentrations measured using identical methods and approaches compared
675 well. Our mean annual Yukon River lignin flux derived for 2001-2009 (5.4 ± 1.7 Gg
676 y^{-1}; Table 5) is similar to previous estimates of 5.3 ± 1.3 Gg y^{-1} independently derived
677 from measurements from 2004-2005 (Spencer et al., 2009), confirming the modeling
678 approach is reproducible and robust. Our estimated lignin loads from all six major
679 arctic rivers (98.4 Gg yr^{-1}) were, however, almost half of the 192.0 Gg yr^{-1} reported by
680 Amon et al., (2012) for the same rivers from 2003 to 2007. These differences were
681 primarily due to the significantly higher lignin concentrations ($\sum_8$) reported by Amon
682 et al., (2012) versus those of Spencer et al., (2009) and reported here, demonstrating
683 the necessity for more standardization and intercomparison across lignin phenol
684 measurements to ensure comparable datasets across studies.
685 Freshwater fluxes were scaled to the unsampled proportion of the Arctic using
686 two published estimates of total Arctic Ocean watershed area. The smallest estimate
687 (PA1; black line Fig. 1) spans an area of 16.8 x 10^6 km^2, where the largest (PA2; red
688 line; Fig. 1) encompassing Hudson Bay drainage covers an area of 20.5 x 10^6 km^2
689 (Hernes et al., 2014). Pan-arctic lignin fluxes were estimated to span between 155.5
690 Gg y^{-1} (PA1) to 185.3 Gg y^{-1} (PA2; Table 5) across these two geographic regions.
691 Dissolved lignin concentrations have previously been applied as a tracer of
692 terrigenous DOM to the Arctic Ocean (Benner et al., 2005; Fichot et al., 2013; Opsahl
693 et al., 1999) and used to estimate turnover rates of terrigenous DOC in the ocean
694 (Hernes and Benner, 2006; Opsahl et al., 1999). Applying our pan-arctic flux (derived
695 using our $lignin_{350}$ proxy) and assuming Arctic Ocean lignin concentrations ranging
696 between 84 to 320 ng L^{-1} (Opsahl et al., 1999), we calculate the residence time of
697 terrigenous DOC in polar surface waters to be in the order of 7 months to 2.5 years.
698 This compares well, yet slightly shorter than residence time estimates of <1 to 4 years

calculated with comparable freshwater fluxes but scaled from the Yukon River alone (Spencer et al., 2009). Assuming the export of lignin phenol concentrations twice as high, similar to those reported by Amon et al., (2012), would result in even faster residence time estimates of < 4 months to 1 year. Overall, the short timeframes identified by these studies indicate either rapid losses of terrigenous DOC, via microbial, photochemical, or flocculation processes, or faster physical transport from Arctic Ocean waters to the North Atlantic than previously thought.

5. Conclusions

Employing optical techniques can increase the temporal and spatial coverage of DOM measurements across arctic river systems, shedding light on future changes in the composition and concentration of exported DOM, and help to more accurately estimate the amount and timing of terrigenous DOC flux. Here, river-specific relationships between a_{350} and DOC concentrations are presented and attributed to the export of varying proportions of non-chromophoric DOM from arctic catchments. We show that simple absorbance proxies (a_{350}, $S_{275\text{-}295}$), which can be measured with *in-situ* techniques, are capable of tracing dissolved lignin concentrations ($\sum_8$) and seasonal changes in geochemical DOM composition (e.g. Λ_8 and percent HPOA) occurring across the six major arctic rivers. Furthermore, we demonstrate that lignin phenol biomarkers appear capable of providing information on the biogeochemical cycling of the hydrophobic DOC fraction, thus knowledge on a major proportion of the aquatic DOM pool. More complex fluorescence DOM measurements followed by PARAFAC decomposition provided few direct pan-arctic proxies of DOM concentration or composition. However, the proportion of fluorescence signatures previously attributed to microbial processing or suggested to be by-products of

724 vascular material degradation co-varied with lignin monomer ratios over much of the
725 year, suggesting these optical measurements may be capable of offering insights into
726 changing DOM degradation state and source. Combining fluorescence and absorbance
727 indices further strengthened our ability to predict DOM composition; in particular,
728 inclusion of fluorescence index and protein-like contributions with absorbance
729 coefficient and spectral slope measurements enabled predictive models of lignin
730 ratios, suggesting potential to distinguish DOM source characteristics. Finally, we
731 combine our pan-arctic relationship between a_{350} and $\sum_8$ with high resolution
732 monitoring of a_{350} to develop more accurately constrained residence times for
733 terrigenous DOC in the Arctic Ocean of between 7 months to 2 ½ years. Optical
734 measurements can provide key insights into the flux and biogeochemical cycling of
735 terrigenous DOC in the Arctic, which will prove critical for understanding how
736 carbon budgets and fluxes alter under future climate change scenarios.
737
738 **Acknowledgments**
739 This work was supported by grants from the National Science Foundation for the
740 Global Rivers Project (0851101), the PARTNERS Project (0229302), the Arctic Great
741 Rivers Observatory I & II (0732522 and 1107774), Detecting the Signature of
742 Permafrost Thaw in Arctic Rivers (1203885 and 1500169), and the US Geological
743 Survey's National Research Program. This work was aided by an NSF equipment
744 grant to upgrade the analytical facilities at the North-East Science Station (0938254).
745 We thank Alexander Shiklomanov for providing additional river discharge data, and
746 the field staff of the USGS Alaska Science Center for their sample collection efforts.
747 Special thanks to Ekaterina Bulygina and Lydia Russell-Roy for help running
748 laboratory analyses. Also thanks to Greg Fiske for production of Figure 1. Any use of
749 trade, firm, or product names is for descriptive purposes only and does not imply

endorsement by the U.S. Government.

Figure legends

Figure 1. Map showing the six Arctic river catchments sampled. Black dots indicate sampling locations. The thick black (PA1) and red lines (PA2) represent two estimates of the total pan-arctic watershed area (16.8 x 10^6 km^2 and 20.5 x 10^6 km^2, respectively).

Figure 2. Seven independent fluorescent components (AG1-7) identified using PARAFAC analysis of 645 excitation-emission matrices. Excitation and emission peak positions are reported alongside descriptions in Table 3.

Figure 3. Panel A: Dissolved organic carbon (DOC) concentration versus the CDOM absorbance coefficient at a_{350} nm from across the hydrograph of the six Arctic rivers. **Panel B:** Lignin phenol concentration ($\sum_8$) versus the CDOM absorbance coefficient at a_{350} nm from across the hydrographs of the six Arctic rivers. Black line represents the linear regression of the data. Thin grey lines represent the extent of the prediction of fit (95 % confidence limit). SS_E indicates the error of the sum of squares providing an indication of variation around the fit.

Figure 4. Panel A: Principle component scores for optical properties across PC1opt and PC2opt for all optical samples labelled by season. **Panel B:** PC scores of each optical parameter across PC1opt and PC2opt. **Panel C:** Principle component scores across PC2opt and PC3opt for all optical samples labelled by season. **Panel D:** PC

775 scores of each optical parameter across PC2opt and PC3opt. FI and $SUVA_{254}$ values
776 were not included in the final optical PCA, see text for details.
777
778 **Figure 5. Panel A:** Principle component scores for geochemical composition (lignin
779 phenol and DOC fractionation variables) across PC1mol and PC2mol for all
780 compositional measurements labelled by season. **Panel B:** PC scores of each
781 compositional parameter across PC1mol and PC2mol. **Panel C:** Principle component
782 scores across PC1mol and PC2mol for all compositional measurements labelled by
783 river. **Panel D:** Relationship between PC2opt derived from optical data alone and
784 PC1mol explaining compositional measurements. Black line represents the linear
785 regression (r^2 = 0.65, p < 0.001).
786
787 **Figure 6.** Model predicted values against measured measurements of: **Panel A:**
788 Carbon normalized sum of the lignin phenols (Λ_8; mg (100 mg OC)$^{-1}$), **Panel B:**
789 Cinnamyl to vanillyl phenol ratios (C/V), and **Panel C:** Syringyl to vanillyl phenol
790 ratios (S/V).

Table 1. Total dissolved organic carbon concentrations (DOC) and major chemical fractions of DOC and fraction-specific ultraviolet absorbance ($SUVA_{254}$) across the six major arctic rivers (mean ± standard error) during Spring (May and June), Summer (July through to October) and Winter (November through to April). Hydrophobic acids (HPOA), transphilic acids (TPI) and hydrophilic organic matter (HPI) presented as percentage of total DOC concentrations and the sample mass of each fraction (HPON comprises the remaining <10 % of the DOC pool).

Site	Season	Total DOC (mgC^{-1})	Total $SUVA_{254}$ ($L\ mgC^{-1}\ m^{-1}$)	HPOA (%)	HPOA $SUVA_{254}$ ($L\ mgC^{-1}\ m^{-1}$)	TPIA (%)	TPIA $SUVA_{254}$ ($L\ mgC^{-1}\ m^{-1}$)	HPI (%)	HPI $SUVA_{254}$ ($L\ mgC^{-1}\ m^{-1}$)
Kolyma	Spring	10.8 ± 1.7	2.9 ± 0.1	54 ± 2	3.9 ± 0.1	16 ± 1	2.4 ± 0.0	21 ± 1	1.5 ± 0.2
	Summer	3.7 ± 0.2	2.5 ± 0.0	56 ± 7	3.4 ± 0.2	18 ± 0	2.2 ± 0.0	20 ± 2	1.7 ± 0.2
	Winter	4.3 ± 1.7	2.0 ± 0.1	50 ± 7	2.9 ± 0.1	18 ± 0	2.0	20	2.1
Lena	Spring	15.7 ± 0.9	3.7 ± 0.0	57 ± 1	4.3 ± 0.0	17 ± 0	2.9 ± 0.0	17 ± 0	1.7 ± 0.0
	Summer	7.4 ± 0.6	2.8 ± 0.4	52 ± 3	4.0 ± 0.4	16 ± 1	2.5 ± 0.1	18 ± 0	1.5 ± 0.1
	Winter	9.7 ± 2.0	2.6 ± 0.3	53 ± 1	3.7 ± 0.1	17 ± 1	2.6 ± 0.1	16 ± 0	1.7 ± 0.2
Mackenzie	Spring	4.7 ± 0.3	2.5 ± 0.6	47 ± 1	3.6 ± 0.2	19 ± 0	2.4 ± 0.1	20 ± 1	1.4 ± 0.1
	Summer	5.4 ± 0.5	2.3 ± .0.1	46 ± 2	3.8 ± 0.2	20 ± 1	2.4 ± 0.1	20 ± 1	1.3 ± 0.0
	Winter	5.1	1.5	40	3.2	16	2.2	24	1.2
Ob’	Spring	9.0 ± 0.4	3.4 ± 0.0	57 ± 1	4.1 ± 0.0	15 ± 1	2.8 ± 0.1	18 ± 1	1.8 ± 0.1
	Summer	11.4 ± 0.9	3.1 ± 0.4	56 ± 1	4.2 ± 0.1	16 ± 1	2.8 ± 0.2	17 ± 1	-
	Winter	9.2 ± 1.9	3.0 ± 0.1	55 ± 3	4.0 ± 0.0	17 ± 1	2.8 ± 0.2	16 ± 1	-
Yenisey	Spring	10.1 ± 0.2	3.9 ± 0.0	60 ± 2	4.4 ± 0.1	16 ± 1	3.1 ± 0.1	16 ± 0	1.7 ± 0.0
	Summer	7.4 ± 1.8	2.8 ± 0.2	49 ± 3	4.2 ± 0.1	17 ± 1	2.6 ± 0.0	22 ± 2	1.5
	Winter	4.7 ± 0.7	2.6 ± 0.2	49 ± 6	3.9 ± 0.2	18 ± 1	2.5 ± 0.1	23 ± 3	2.3
Yukon	Spring	9.8 ± 2.3	3.2 ± 0.1	53 ± 1	4.2 ± 0.1	15 ± 0	2.8 ± 0.0	19 ± 1	2.2 ± 0.2
	Summer	7.1 ± 1.5	2.5 ± 0.2	50 ± 2	4.0 ± 0.4	19 ± 1	2.6 ± 0.1	21 ± 2	1.9 ± 0.2
	Winter	2.9	2	43	3.3	18	2.1	22	2.2

Table 2. Sampling location and date of discharge (Q), dissolved organic carbon (DOC) and lignin phenol concentration ($\sum_8$), carbon normalized sum of lignin yields (Λ_8), lignin ratios (C/V and S/V) and acid aldehyde ratios (Ad/Al) measurements; ratios of vanillic acid to vanillin (Ad/Al)v and ratios of syringic acid to syringaldehyde (Ad/Al)s. Site-normalized discharge (Q) is also presented.

River	Date	Q ($m^3 s^{-1}$)	DOC (mgC L^{-1})	$\sum_8$ (μg L^{-1})	Λ_8 (mg(100 mg OC))$^{-1}$	C/V	S/V	(Ad/Al)v	(Ad/Al)s
Kolyma	05 Jun 2009	12,800	10.7	54.2	0.51	0.16	0.51	1.58	1.14
Kolyma	12 Jun 2009	11,100	9.1	45.1	0.50	0.18	0.58	1.42	1.00
Kolyma	21 Jun 2009	8,270	5.5	16.8	0.31	0.18	0.41	1.29	1.06
Kolyma	09 Sep 2009	8,390	3.9	17.0	0.44	0.19	0.64	1.51	1.08
Kolyma	08 Nov 2009	3,850	2.6	3.8	0.15	0.24	0.47	1.41	1.02
Lena	31 May 2009	68,328	17.5	120.0	0.69	0.04	0.17	1.28	0.98
Lena	05 Jun 2009	128,769	16.7	107.2	0.65	0.05	0.19	1.28	0.94
Lena	11 Jun 2009	83,800	12.9	85.2	0.66	0.07	0.25	1.30	0.96
Lena	22 Aug 2009	33,400	6.8	20.9	0.31	0.14	0.28	1.36	1.05
Lena	18 Nov 2009	4,102	7.7	16.5	0.22	0.12	0.30	1.34	1.09
Mackenzie	11 Jun 2009	24,300	4.3	16.2	0.38	0.17	0.34	1.01	0.81
Mackenzie	30 Jun 2009	20,900	5.3	9.3	0.18	0.28	0.50	1.24	1.38
Mackenzie	02 Jul 2009	21,100	6.6	8.3	0.13	0.19	0.43	0.98	0.89
Mackenzie	08 Sep 2009	13,800	5.0	8.0	0.16	0.18	0.37	1.06	1.00
Mackenzie	25 Mar 2010	4,380	5.1	5.5	0.11	0.32	0.51	1.09	1.13
Ob'	02 Jun 2009	36,300	8.1	55.5	0.69	0.23	0.61	1.39	0.93
Ob'	07 Jun 2009	36,100	8.5	40.4	0.48	0.19	0.58	1.39	0.89
Ob'	13 Jun 2009	35,400	7.7	55.7	0.73	0.19	0.59	1.38	0.88
Ob'	25 Aug 2009	13,500	10.5	22.4	0.22	0.20	0.46	0.93	0.90
Ob'	01 Dec 2009	5,152	7.3	17.2	0.24	0.31	0.68	0.97	0.75
Yenisey	17 Jun 2009	85,400	9.8	71.2	0.73	0.07	0.29	1.39	0.91
Yenisey	21 Jun 2009	67,200	9.5	74.7	0.79	0.08	0.29	1.40	0.86

Yenisey	27 Jun 2009	45,600	9.6	57.6	0.60	0.07	0.26	1.17	0.77
Yenisey	08 Aug 2009	15,200	5.6	18.7	0.33	0.15	0.37	0.99	0.80
Yenisey	30 Nov 2009	11,167	4.0	12.2	0.31	0.18	0.35	0.84	0.88
Yukon	14 May 2009	11,836	5.2	17.2	0.34	0.10	0.57	1.70	1.05
Yukon	20 May 2009	10,874	13.0	62.1	0.48	0.11	0.48	1.90	1.03
Yukon	26 May 2009	26,901	15.0	95.5	0.64	0.13	0.54	1.79	1.28
Yukon	07 Jul 2009	15,008	5.6	11.5	0.21	0.15	0.46	0.99	0.77
Yukon	18 Aug 2009	7,759	2.6	4.2	0.16	0.27	0.51	1.02	0.77
Yukon	12 Jan 2010	1,869	2.9	3.8	0.13	0.33	0.63	1.10	1.14

Table 3. Excitation and emission maxima (Ex_{max}/ Em_{max}) of the seven components identified using parallel factor analysis of DOM fluorescence (Fig. 2). Description of previously identified components displaying similar optical properties (TCC > 0.95; see text for details). *ID number refers to assigned study number in OpenFluor (http://www.openfluor.org).

Component	Ex_{max} (nm)	Em_{max} (nm)	Comparable study ID* (component with TCC >0.95)	Description
AG1	265	492	7 (C3), 8 (C2), 28 (C2), 31 (C4), 37 (C3), 44 (C2), 48 (C2), 54 (C2)	Humic-like fluorophore, terrigenous or autochthonous source, fulvic acid-like, present in all environments; Positively related to agriculture and bacterial production. Identified in many models and possibly formed as intermediate during photochemical degradation. Susceptible to microbial degradation.
AG2	270	448	29 (C5), 31 (C3), 69 (C4)	Similar to classical 'C peak'. Terrigenous component identified across a range of environments.
AG3	315	434	8 (C1)	Humic-like, emission spectum identical to syringaldehyde (producted in breakdown of lignin) associated with waters containing high DOM loadings.
AG4	365	444	22 (C3), 34 (C1), 41 (C2), 47 (C2), 53 (C5), 55 (C3)	Similar to classical 'A peak' , Terrigenous humic-like substances, refractory in nature.
AG5	320	392	8 (C4), 22 (C2), 26 (C6), 32 (C4), 47 (C3), 68 (C2)	Similar to classical 'M peak', marine and terrigenous humic material source, possibly derived from microbial reprocessing.
AG6	305	424	9 (C1), 28 (C3), 35 (C1), 44 (C3), 48 (C1), 54 (C3), 64 (C1)	Humic-like fluorophore, terrigenous; not correlated with land use or bacterial production
AG7	280	364	8 (C5), 9 (C7), 33 (C5), 34 (C7), 35 (C5), 39 (C5), 64 (C5)	Tryptophan-like associated with biological production in surface waters. Also a region known to be associated with phenolic fluorescence.

ID*: [7][Murphy et al., 2006], [8][Murphy et al., 2014], [9][Murphy et al., 2008], [22][Kothawala et al., 2012], [26][Stedmon et al., 2011b], [28][Stedmon et al., 2007], [29][Stedmon and Markager, 2005], [31][Søndergaard et al., 2003], [32][Jørgensen et al., 2011], [33][Stedmon et al., 2003], [34][Stedmon and Markager, 2005], [35][Osburn and Stedmon, 2011], [37][Walker et al., 2009], [39][Yamashita et al., 2011], [41][Yamashita et al., 2010a], [44][Yamashita et al., 2010b], [47][Kowalczuk et al., 2009], [48][Graeber et al., 2012], [53][Kothawala et al., 2013], [54][Osburn et al., 2012], [55][Osburn et al., 2011], [64][Walker et al., 2013], [68][Tanaka et al., 2014], [69][Lapierre and del Giorgio, 2014].

Table 4. Linear regression fits for linear relationships between dissolved organic carbon concentration (DOC) and absorbance coefficient (a_{350}) determined for each river. *n* represents number of measurements, R^2 the coefficient of determination and SE_E the standard error of the mean. [a]Annual average discharge from each river from Holmes et al. (2012).

River	*n*	R^2	slope	intercept	SE_E (%)	Discharge[a] ($km^3\ y^{-1}$)
Kolyma	23	0.84	0.478 ± 0.045	0.845 ± 1.022	2.0	111
Lena	57	0.83	0.333 ± 0.020	3.429 ± 0.666	1.5	581
Mackenzie	60	0.86	0.310 ±0.017	3.871 ± 0.256	0.9	298
Ob'	54	0.74	0.295 ± 0.024	2.240 ± 0.531	1.0	427
Yenisey	58	0.66	0.231 ± 0.022	3.793 ± 0.528	0.8	636
Yukon	49	0.95	0.405 ± 0.014	1.346 ± 0.310	1.0	208
ALL	301	0.81	0.343 ± 0.009	2.414 ± 0.229	1.6	2261

Table 5. Total annual mean fluxes of CDOM-derived lignin ($Lignin_{350}$) and DOC calculated using LOADEST. Arctic-GRO refers to the sum of all 6 rivers studied, and pan-arctic1 & 2 are the regions delineated in Figure 1. Mean annual discharge is calculated for the 1999 – 2010 period. [#]Averaged over 2001 – 2010.

River/ region	Watershed Area (10^6 km^2)	Discharge (km^3 y^{-1})	$Lignin_{350}$ (Gg y^{-1})		
			2009	2010	1999-2010
Kolyma	0.65	132	3.6	3.2	5.0 ± 1.2
Lena	2.4	591	50.5	36.2	43.1 ± 8.6
Mackenzie	1.75	319	5.2	3.5	4.0 ± 1.0
Ob'	2.95	421	15.5	16.2	18.6 ± 4.8
Yenisey	2.56	671	20.9	21.9	22.3 ± 2.3
Yukon	0.83	207	4.6	6.3	5.4 ± 1.7[#]
Arctic-GRO	11.14	2342	100.3	87.3	98.4
pan-arctic1 (PA1)	16.8	3700	158.5	137.9	155.5
pan-arctic2 (PA2)	20.5	4410	188.9	164.4	185.3

References.

Aagaard, K., and Carmack, E. C. (1989). The role of sea ice and other fresh water in the Arctic circulation. *Journal of Geophysical Research: Atmospheres (1984–2012)* 94, 14485–14498. doi:10.1029/JC094iC10p14485.

Aiken, G. R., McKnight, D. M., Thorn, K. A., and Thurman, E. M. (1992). Isolation of hydrophilic organic acids from water using nonionic macroporous resins. *Organic Geochemistry* 18, 567–573. doi:10.1016/0146-6380(92)90119-I.

Amon, R. M. W., Rinehart, A. J., Duan, S., Louchouarn, P., Prokushkin, A., Guggenberger, G., et al. (2012). Dissolved organic matter sources in large Arctic rivers. *Geochimica et Cosmochimica Acta* 94, 217–237. doi:10.1016/j.gca.2012.07.015.

Benner, R., Louchouarn, P., and Amon, R. M. W. (2005). Terrigenous dissolved organic matter in the Arctic Ocean and its transport to surface and deep waters of the North Atlantic. *Global Biogeochem. Cycles* 19, GB2025 doi:10.1029/2004GB002398.

Blough, N. V., and Del Vecchio, R. (2002). "Chromophoric DOM in the coastal environment," in *Biogeochemistry of Marine Dissolved Organic Matter*, eds.D. A. Hansell and C. A. Carlson, 509–546.

Blough, N. V., and Green, S. A. (1995). "Spectroscopic characterization and remote sensing of non-living organic matter," in *The Role of Non-Living Organic Matter on the Earths Carbon Cycle*, eds. R. G. Zepp and C. Sonntag, 23–45.

Booth, G. P., Raymond, P. A., and Oh, N. H. (2007) LoadRunner. Software and website. Yale University: New Haven. http://research.yale.edu/environment/loadrunner/.

Coble, P. G. (1996). Characterization of marine and terrestrial DOM in seawater using excitation-emission matrix spectroscopy. *Marine Chemistry* 51, 325–346. doi:10.1016/0304-4203(95)00062-3.

Coble, P. G. (2007). Marine optical biogeochemistry: the chemistry of ocean color. *Chem. Rev.* 107, 402–418. doi:10.1021/cr050350.

Cory, R. M., Miller, M. P., and McKnight, D. M. (2010). Effect of instrument-specific response on the analysis of fulvic acid fluorescence spectra. *Limnology and Oceanography: Methods*. 67-78. doi:10.4319/lom.2010.8.67.

Determann, S., Reuter, R., Wagner, P., and Willkomm, R. (1994). Fluorescent matter in the eastern Atlantic Ocean. Part 1: method of measurement and near-surface distribution. *Deep Sea Research Part I: Oceanographic Research Papers* 41, 659–675.

Déry, S. J., Stahl, K., Moore, R. D., Whitfield, P. H., Menounos, B., and Burford, J. E. (2009). Detection of runoff timing changes in pluvial, nival, and glacial rivers

of western Canada. *Water Resour. Res.* 45, W04426. doi:10.1029/2008WR006975.

Fellman, J. B., Hood, E., and Spencer, R. G. M. (2010). Fluorescence spectroscopy opens new windows into dissolved organic matter dynamics in freshwater ecosystems: A review. *Limnol. Oceangr.* 55, 2452–2462. doi:10.4319/lo.2010.55.6.2452.

Fichot, C. G., Kaiser, K., Hooker, S. B., Amon, R. M. W., Babin, M., Bélanger, S., et al. (2013). Pan-Arctic distributions of continental runoff in the Arctic Ocean. *Sci. Rep.* 3, 1053. doi:10.1038/srep01053.

Graeber, D., Gelbrecht, J., Pusch, M. T., Anlanger, C., and Schiller, von, D. (2012). Agriculture has changed the amount and composition of dissolved organic matter in Central European headwater streams. *Science of the Total Environment,* 438, 435–446. doi:10.1016/j.scitotenv.2012.08.087.

Harshman, R. A., and Lundy, M. E. (1994). PARAFAC: Parallel factor analysis. *Computational Statistics & Data Analysis* 18, 39–72. doi:10.1016/0167-9473(94)90132-5.

Hedges, J. I., and Ertel, J. R. (1982). Characterization of lignin by gas capillary chromatography of cupric oxide oxidation products. *Analytical Chemistry* 54, 174–178. doi:10.1021/ac00239a007.

Hedges, J. I., and Mann, D. C. (1979). The characterization of plant tissues by their lignin oxidation products. *Geochimica et Cosmochimica Acta* 43, 1803–1807.

Hedges, J. I., Clark, W. A., and Cowie, G. L. (1988). Organic matter sources to the water column and surficial sediments of a marine bay. *Limnol. Oceangr.* 33, 1116–1136. doi:10.4319/lo.1988.33.5.1116.

Helms, J. R., Stubbins, A., and Ritchie, J. D. (2008). Absorption spectral slopes and slope ratios as indicators of molecular weight, source, and photobleaching of chromophoric dissolved organic matter. *Limnology and Oceanography: Methods* 53, 955–969.

Hernes, P. J., and Benner, R. (2003). Photochemical and microbial degradation of dissolved lignin phenols: Implications for the fate of terrigenous dissolved organic matter in marine environments. *J. Geophys. Res.* 108, 3291. doi:10.1029/2002JC001421.

Hernes, P. J., and Benner, R. (2006). Terrigenous organic matter sources and reactivity in the North Atlantic Ocean and a comparison to the Arctic and Pacific oceans. *Marine Chemistry* 100, 66–79. doi:10.1016/j.marchem.2005.11.003.

Hernes, P. J., Bergamaschi, B. A., Eckard, R. S., and Spencer, R. G. M. (2009). Fluorescence-based proxies for lignin in freshwater dissolved organic matter. *J. Geophys. Res.* 114, G00F03–10. doi:10.1029/2009JG000938.

Hernes, P. J., Holmes, R. M., Raymond, P. A., Spencer, R. G. M., and Tank, S. E. (2014). “Fluxes, processing, and fate of riverine organic and inorganic carbon in

the Arctic Ocean," in *Biogeochemical Dynamics at Major River-Coastal Interfaces：Linkages with Global Change*, eds. T. S. Bianchi, M. A. Allison and W-J. Cai, 530–553. doi:10.1017/CBO9781139136853.026.

Hernes, P. J., Robinson, A. C., and Aufdenkampe, A. K. (2007). Fractionation of lignin during leaching and sorption and implications for organic matter "freshness." *Geophysical Research Letters* 34, L17401–6. doi:10.1029/2007GL031017.

Hernes, P. J., Spencer, R. G. M., Dyda, R. Y., Pellerin, B. A., Bachand, P. A. M., and Bergamaschi, B. A. (2008). The role of hydrologic regimes on dissolved organic carbon composition in an agricultural watershed. *Geochimica et Cosmochimica Acta* 72, 5266–5277. doi:10.1016/j.gca.2008.07.031.

Holmes, R. M., McClelland, J. W., Peterson, B. J., Tank, S. E., Bulygina, E., Eglinton, T. I., et al. (2012). Seasonal and Annual Fluxes of Nutrients and Organic Matter from Large Rivers to the Arctic Ocean and Surrounding Seas. *Estuaries and Coasts* 35, 369–382. doi:10.1007/s12237-011-9386-6.

Holmes, R. M., McClelland, J. W., Raymond, P. A., Frazer, B. B., Peterson, B. J., and Stieglitz, M. (2008). Lability of DOC transported by Alaskan rivers to the Arctic Ocean. *Geophysical Research Letters* 35, L03402–5. doi:10.1029/2007GL032837.

Hu, C., Muller-Karger, F. E., and Zepp, R. G. (2002). Absorbance, absorption coefficient, and apparent quantum yield: A comment on common ambiguity in the use of these optical concepts. *Limnol. Oceangr.* 47, 1261–1267. doi:10.4319/lo.2002.47.4.1261.

Jørgensen, L., Stedmon, C. A., Kragh, T., Markager, S., Middelboe, M., and Søndergaard, M. (2011). Global trends in the fluorescence characteristics and distribution of marine dissolved organic matter. *Marine Chemistry* 126, 139–148. doi:10.1016/j.marchem.2011.05.002.

Köhler, H., Meon, B., Gordeev, V. V., Spitzy, A., and Amon, R. M. W. (2003). "Dissolved organic matter (DOM) in the estuaries of Ob and Yenisei and the adjacent Kara Sea, Russia," in *Siberian river run-off in the Kara Sea*, eds.R. Stein, K. Fahl, D. K. Fütterer, E. M. Galimov, and O. V. Stepanets.

Kothawala, D. N., Stedmon, C. A., Müller, R. A., Weyhenmeyer, G. A., Köhler, S. J., and Tranvik, L. J. (2013). Controls of dissolved organic matter quality: Evidence from a large-scale boreal lake survey. *Global Change Biology* 20, 1101–1114. doi:10.1111/gcb.12488.

Kothawala, D. N., Wachenfeldt, von, E., Koehler, B., and Tranvik, L. J. (2012). Selective loss and preservation of lake water dissolved organic matter fluorescence during long-term dark incubations. *Science of the Total Environment,* 433, 238–246. doi:10.1016/j.scitotenv.2012.06.029.

Kowalczuk, P., Durako, M. J., Young, H., Kahn, A. E., Cooper, W. J., and Gonsior, M. (2009). Characterization of dissolved organic matter fluorescence in the South

Atlantic Bight with use of PARAFAC model: Interannual variability. *Marine Chemistry* 113, 182–196. doi:10.1016/j.marchem.2009.01.015.

Lakowicz, J. R. (2013). *Principles of Fluorescence Spectroscopy*. Springer Science & Business Media doi:10.1007/978-0-387-46312-4.

Lapierre, J.-F., and del Giorgio, P. A. (2014). Partial coupling and differential regulation of biologically and photochemically labile dissolved organic carbon across boreal aquatic networks. *Biogeosciences* 11, 5969–5985. doi:10.5194/bg-11-5969-2014.

Lawaetz, A. J., and Stedmon, C. A. (2009). Fluorescence intensity calibration using the Raman Scatter Peak of water. *Appl Spectrosc* 63, 936–940. doi:10.1366/000370209788964548.

Lobbes, J. M., Fitznar, H. P., and Kattner, G. (2000). Biogeochemical characteristics of dissolved and particulate organic matter in Russian rivers entering the Arctic Ocean. *Geochimica et Cosmochimica Acta* 64, 2973–2983.

Mann, P. J., Davydova, A., Zimov, N., Spencer, R. G. M., Davydov, S., Bulygina, E., et al. (2012). Controls on the composition and lability of dissolved organic matter in Siberia's Kolyma River basin. *J. Geophys. Res.* 117, G01028. doi:10.1029/2011jg001798.

Mann, P. J., Eglinton, T. I., McIntyre, C. P., Zimov, N., Davydova, A., Vonk, J. E., et al. (2015). Utilization of ancient permafrost carbon in headwaters of Arctic fluvial networks. *Nature Communications* 6, 7856. doi:10.1038/ncomms8856.

Mann, P. J., Spencer, R. G. M., Dinga, B. J., Poulsen, J. R., Hernes, P. J., Fiske, G., et al. (2014). The biogeochemistry of carbon across a gradient of streams and rivers within the Congo Basin. *J. Geophys. Res. Biogeosci.* 119, 687–702. doi:10.1002/(ISSN)2169-8961.

Mathis, J. T., Hansell, D. A., and Bates, N. R. (2005). Strong hydrographic controls on spatial and seasonal variability of dissolved organic carbon in the Chukchi Sea. *Deep Sea Research Part II: Topical Studies in Oceanography* 52, 3245–3258. doi:10.1016/j.dsr2.2005.10.002.

McClelland, J. W., Déry, S. J., Peterson, B. J., Holmes, R. M., and Wood, E. F. (2006). A pan-arctic evaluation of changes in river discharge during the latter half of the 20th century. *Geophysical Research Letters* 33, L06715–4. doi:10.1029/2006GL025753.

McClelland, J. W., Holmes, R. M., Dunton, K. H., and Macdonald, R. W. (2011). The Arctic Ocean Estuary. *Estuaries and Coasts* 35, 353–368. doi:10.1007/s12237-010-9357-3.

McClelland, J. W., Holmes, R. M., Peterson, B. J., Amon, R. M. W., Brabets, T., Cooper, L. W., et al. (2008). Development of a Pan-Arctic Database for River Chemistry. *Eos*. 89, 24, 217-218. doi:10.1029/2005JG000031.

McKnight, D. M., Boyer, E. W., Westerhoff, P. K., Doran, P. T., Kulbe, T., and

Andersen, D. T. (2001). Spectrofluorometric characterization of dissolved organic matter for indication of precursor organic material and aromaticity. *Limnol. Oceangr.* 46, 38–48. doi:10.4319/lo.2001.46.1.0038.

Murphy, K. R., Bro, R., and Stedmon, C. A. (2014). "Chemometric analysis of organic matter fluorescence," in *Aquatic Organic Matter Fluorescence*, eds.P. Coble, J. Lead, A. Baker, D. Reynolds, and R. G. M. Spencer, 339–375. doi:10.13140/2.1.2595.8080.

Murphy, K. R., Ruiz, G. M., Dunsmuir, W. T. M., and Waite, T. D. (2006). Optimized parameters for fluorescence-based verification of ballast water exchange by ships. *Environ. Sci. Technol.* 40, 2357–2362. doi:10.1021/es0519381.

Murphy, K. R., Stedmon, C. A., Graeber, D., and Bro, R. (2013). Fluorescence spectroscopy and multi-way techniques. PARAFAC. *Anal. Methods* 5, 6557–6566. doi:10.1039/c3ay41160e.

Murphy, K. R., Stedmon, C. A., Waite, T. D., and Ruiz, G. M. (2008). Distinguishing between terrestrial and autochthonous organic matter sources in marine environments using fluorescence spectroscopy. *Marine Chemistry* 108, 40–58. doi:10.1016/j.marchem.2007.10.003.

Neff, J. C., Finlay, J. C., Zimov, S. A., Davydov, S. P., Carrasco, J. J., Schuur, E. A. G., et al. (2006). Seasonal changes in the age and structure of dissolved organic carbon in Siberian rivers and streams. *Geophysical Research Letters* 33, L23401. doi:10.1029/2006GL028222.

O'Donnell, J. A., Aiken, G. R., Walvoord, M. A., and Butler, K. D. (2012). Dissolved organic matter composition of winter flow in the Yukon River basin: Implications of permafrost thaw and increased groundwater discharge. *Global Biogeochem. Cycles* 26, 4. doi:10.1029/2012GB004341.

Opsahl, S., and Benner, R. (1995). Early diagenesis of vascular plant tissues: Lignin and cutin decomposition and biogeochemical implications. *Geochimica et Cosmochimica Acta* 59, 4889–4904. doi:10.1016/0016-7037(95)00348-7.

Opsahl, S., Benner, R., and Amon, R. M. W. (1999). Major flux of terrigenous dissolved organic matter through the Arctic Ocean. *Limnol. Oceangr.* 44, 2017–2023. doi:10.4319/lo.1999.44.8.2017.

Osburn, C. L., Handsel, L. T., Mikan, M. P., Paerl, H. W., and Montgomery, M. T. (2012). Fluorescence Tracking of Dissolved and Particulate Organic Matter Quality in a River-Dominated Estuary. *Environ. Sci. Technol.* 46, 8628–8636. doi:10.1021/es3007723.

Osburn, C. L., and Stedmon, C. A. (2011). Linking the chemical and optical properties of dissolved organic matter in the Baltic–North Sea transition zone to differentiate three allochthonous inputs. *Marine Chemistry* 126, 281–294. doi:10.1016/j.marchem.2011.06.007.

Osburn, C. L., Wigdahl, C. R., Fritz, S. C., and Saros, J. E. (2011). Dissolved organic

matter composition and photoreactivity in prairie lakes of the U.S. Great Plains. *Limnol. Oceangr.* 56, 2371–2390. doi:10.4319/lo.2011.56.6.2371.

Peterson, B. J. (2002). Increasing river discharge to the Arctic Ocean. *Science* 298, 2171–2173. doi:10.1126/science.1077445.

Rawlins, M. A., Steele, M., Holland, M. M., Adam, J. C., Cherry, J. E., Francis, J. A., et al. (2010). Analysis of the Arctic system for freshwater cycle intensification: Observations and expectations. *J. Climate* 23, 5715–5737. doi:10.1175/2010JCLI3421.1.

Raymond, P. A., McClelland, J. W., Holmes, R. M., Zhulidov, A. V., Mull, K., Peterson, B. J., et al. (2007). Flux and age of dissolved organic carbon exported to the Arctic Ocean: A carbon isotopic study of the five largest arctic rivers. *Global Biogeochem. Cycles* 21, 4. doi:10.1029/2007GB002934.

Romanovsky, V. E., Drozdov, D. S., Oberman, N. G., Malkova, G. V., Kholodov, A. L., Marchenko, S. S., et al. (2010). Thermal state of permafrost in Russia. *Permafrost Periglac. Process.* 21, 136–155. doi:10.1002/ppp.683.

Runkel, R. L., Crawford, C. G., and Cohn, T. A. (2004). LoadEstimator (LOADEST): A FORTRAN Program for estimating constituent loads in streams and rivers, In U.S. Geological Survey Techniques and Methods, Book 4, Chapter A5, 69

Serreze, M. C., Barrett, A. P., Slater, A. G., Woodgate, R. A., Aagaard, K., Lammers, R. B., et al. (2006). The large-scale freshwater cycle of the Arctic. *J. Geophys. Res.* 111, C11010–19. doi:10.1029/2005JC003424.

Smith, L. C., Pavelsky, T. M., MacDonald, G. M., Shiklomanov, A. I., and Lammers, R. B. (2007). Rising minimum daily flows in northern Eurasian rivers: A growing influence of groundwater in the high-latitude hydrologic cycle. *J. Geophys. Res.* 112, G04S47. doi:10.1029/2006JG000327.

Søndergaard, M., Stedmon, C. A., and Borch, N. H. (2003). Fate of terrigenous dissolved organic matter (DOM) in estuaries: Aggregation and bioavailability. *Ophelia* 57, 161–176. doi:10.1080/00785236.2003.10409512.

Spencer, R. G. M., Aiken, G. R., Butler, K. D., Dornblaser, M. M., Striegl, R. G., and Hernes, P. J. (2009). Utilizing chromophoric dissolved organic matter measurements to derive export and reactivity of dissolved organic carbon exported to the Arctic Ocean: A case study of the Yukon River, Alaska. *Geophysical Research Letters* 36, L06401–6. doi:10.1029/2008GL036831.

Spencer, R. G. M., Aiken, G. R., Dyda, R. Y., Butler, K. D., Bergamaschi, B. A., and Hernes, P. J. (2010b). Comparison of XAD with other dissolved lignin isolation techniques and a compilation of analytical improvements for the analysis of lignin in aquatic settings. *Organic Geochemistry* 41, 445–453. doi:10.1016/j.orggeochem.2010.02.004.

Spencer, R. G. M., Aiken, G. R., Wickland, K. P., Striegl, R. G., and Hernes, P. J. (2008). Seasonal and spatial variability in dissolved organic matter quantity and

composition from the Yukon River basin, Alaska. *Global Biogeochem. Cycles* 22, 4. doi:10.1029/2008GB003231.

Spencer, R. G. M., Butler, K. D., and Aiken, G. R. (2012). Dissolved organic carbon and chromophoric dissolved organic matter properties of rivers in the USA. *J. Geophys. Res.* 117, G03001–14. doi:10.1029/2011JG001928.

Spencer, R. G. M., Hernes, P. J., Ruf, R., Baker, A., Dyda, R. Y., Stubbins, A., et al. (2010a). Temporal controls on dissolved organic matter and lignin biogeochemistry in a pristine tropical river, Democratic Republic of Congo. *J. Geophys. Res.* 115, G03013. doi:10.1029/2009JG001180.

Spencer, R. G. M., Mann, P. J., Dittmar, T., Eglinton, T. I., McIntyre, C., Holmes, R. M., et al. (2015). Detecting the signature of permafrost thaw in Arctic rivers. *Geophysical Research Letters* 42, 2830–2835. doi:10.1002/2015GL063498.

Stedmon, C. A., Amon, R., Rinehart, A. J., and Walker, S. A. (2011a). The supply and characteristics of colored dissolved organic mater (CDOM) in the Arctic Ocean: Pan Arctic trends and differences. *Marine Chemistry* 124, 108–118. doi:10.1016/j.marchem.2010.12.007.

Stedmon, C. A., and Markager, S. (2005). Resolving the variability in dissolved organic matter fluorescence in a temperate estuary and its catchment using PARAFAC analysis. *Limnol. Oceangr.* 50, 686–697. doi:10.4319/lo.2005.50.2.0686.

Stedmon, C. A., Markager, S., and Bro, R. (2003). Tracing dissolved organic matter in aquatic environments using a new approach to fluorescence spectroscopy. *Marine Chemistry* 82, 239–254. doi:10.1016/S0304-4203(03)00072-0.

Stedmon, C. A., Thomas, D. N., Granskog, M., Kaartokallio, H., Papadimitriou, S., and Kuosa, H. (2007). Characteristics of dissolved organic matter in Baltic coastal sea ice: Allochthonous or autochthonous origins? *Environ. Sci. Technol.* 41, 7273–7279. doi:10.1021/es071210f.

Stedmon, C. A., Thomas, D. N., Papadimitriou, S., Granskog, M. A., and Dieckmann, G. S. (2011b). Using fluorescence to characterize dissolved organic matter in Antarctic sea ice brines. *J. Geophys. Res.* 116, G03027–9. doi:10.1029/2011JG001716.

Striegl, R. G., Aiken, G. R., Dornblaser, M. M., Raymond, P. A., and Wickland, K. P. (2005). A decrease in discharge-normalized DOC export by the Yukon River during summer through autumn. *Geophysical Research Letters* 32, L21413. doi:10.1029/2005GL024413.

Striegl, R. G., Dornblaser, M. M., Aiken, G. R., Wickland, K. P., and Raymond, P. A. (2007). Carbon export and cycling by the Yukon, Tanana, and Porcupine rivers, Alaska, 2001-2005. *Water Resour. Res.* 43, 2. doi:10.1029/2006WR005201.

Tanaka, K., Kuma, K., Hamasaki, K., and Yamashita, Y. (2014). Accumulation of humic-like fluorescent dissolved organic matter in the Japan Sea. *Sci. Rep.* 4, 1–7.

doi:10.1038/srep05292.

Tarnocai, C., Canadell, J. G., Schuur, E. A. G., Kuhry, P., Mazhitova, G., and Zimov, S. (2009). Soil organic carbon pools in the northern circumpolar permafrost region. *Global Biogeochem. Cycles* 23, 2. doi:10.1029/2008GB003327.

Templier, J., Derenne, S., Croué, J.-P., and Largeau, C. (2005). Comparative study of two fractions of riverine dissolved organic matter using various analytical pyrolytic methods and a 13C CP/MAS NMR approach. *Organic Geochemistry* 36, 1418–1442. doi:10.1016/j.orggeochem.2005.05.003.

Tucker, L. R. (1951). *A method for synthesis of factor analysis studies* (Personnel Research Section Report No. 984). Washington, DC: Department of the Army.

Walker, S. A., Amon, R. M. W., and Stedmon, C. A. (2013). Variations in high-latitude riverine fluorescent dissolved organic matter: A comparison of large Arctic rivers. *J. Geophys. Res. Biogeosci.*, 118, 4, 1689-1702. doi:10.1002/2013JG002320.

Walker, S. A., Amon, R. M. W., Stedmon, C. A., Duan, S., and Louchouarn, P. (2009). The use of PARAFAC modeling to trace terrestrial dissolved organic matter and fingerprint water masses in coastal Canadian Arctic surface waters. *J. Geophys. Res.* 114, G00F06–12. doi:10.1029/2009JG000990.

Weishaar, J. L., Aiken, G. R., Bergamaschi, B. A., Fram, M. S., Fujii, R., and Mopper, K. (2003). Evaluation of specific ultraviolet absorbance as an indicator of the chemical composition and reactivity of dissolved organic carbon. *Environ. Sci. Technol.* 37, 4702–4708. doi:10.1021/es030360x.

Wickland, K. P., Aiken, G. R., Butler, K., Dornblaser, M. M., Spencer, R. G. M., and Striegl, R. G. (2012). Biodegradability of dissolved organic carbon in the Yukon River and its tributaries: Seasonality and importance of inorganic nitrogen. *Global Biogeochem. Cycles* 26, 4. doi:10.1029/2012GB004342.

Yamashita, Y., Kloeppel, B. D., Knoepp, J., Zausen, G. L., and Jaffé, R. (2011). Effects of watershed history on dissolved organic matter characteristics in headwater streams. *Ecosystems* 14, 1110–1122. doi:10.1007/s10021-011-9469-z.

Yamashita, Y., Maie, N., Briceño, H., and Jaffé, R. (2010b). Optical characterization of dissolved organic matter in tropical rivers of the Guayana Shield, Venezuela. *J. Geophys. Res.* 115, G00F10–15. doi:10.1029/2009JG000987.

Yamashita, Y., Scinto, L. J., Maie, N., and Jaffé, R. (2010a). Dissolved organic matter characteristics across a subtropical wetland's landscape: Application of optical properties in the assessment of environmental dynamics. *Ecosystems* 13, 1006–1019. doi:10.1007/s10021-010-9370-1.

Figure 1.TIF


Pacific
Ocean
Yukon
Kolyma
Mackenzie
Lena
Yenisey
Arctic
Ocean
Ob'
75°N
60°N
Atlantic
Ocean
45°N

Figure 2.TIF

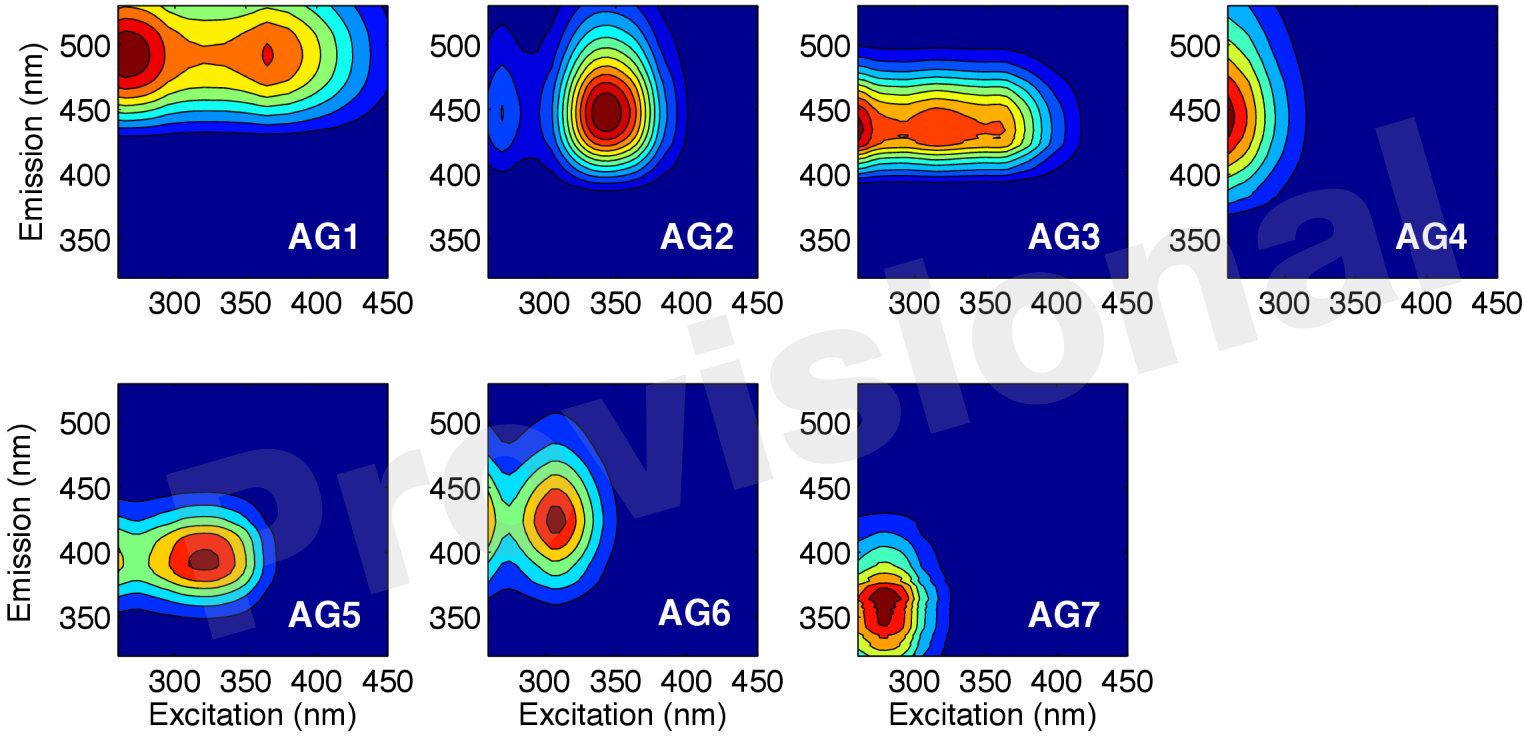

Figure 3.TIF

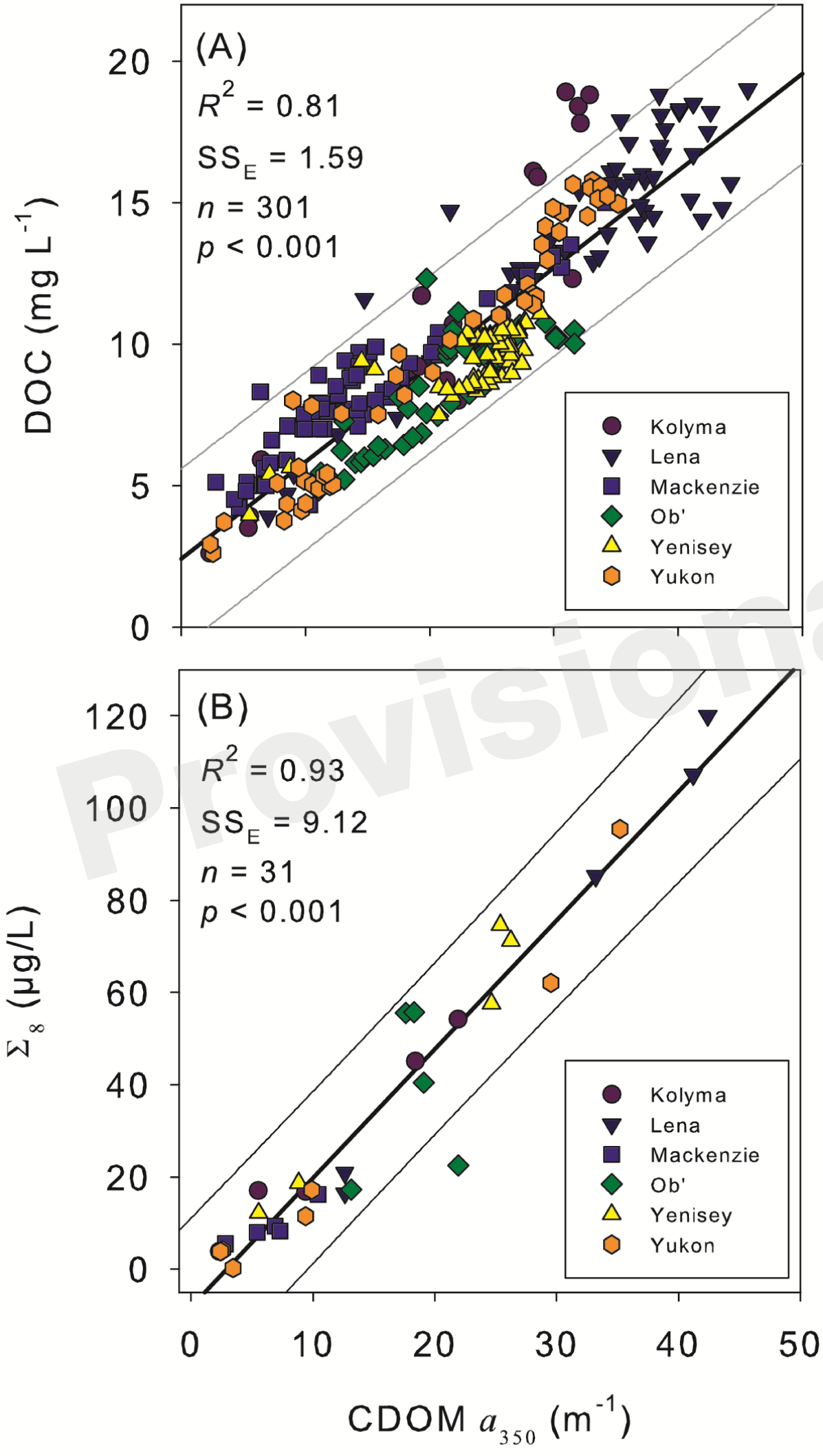

Figure 4.TIF

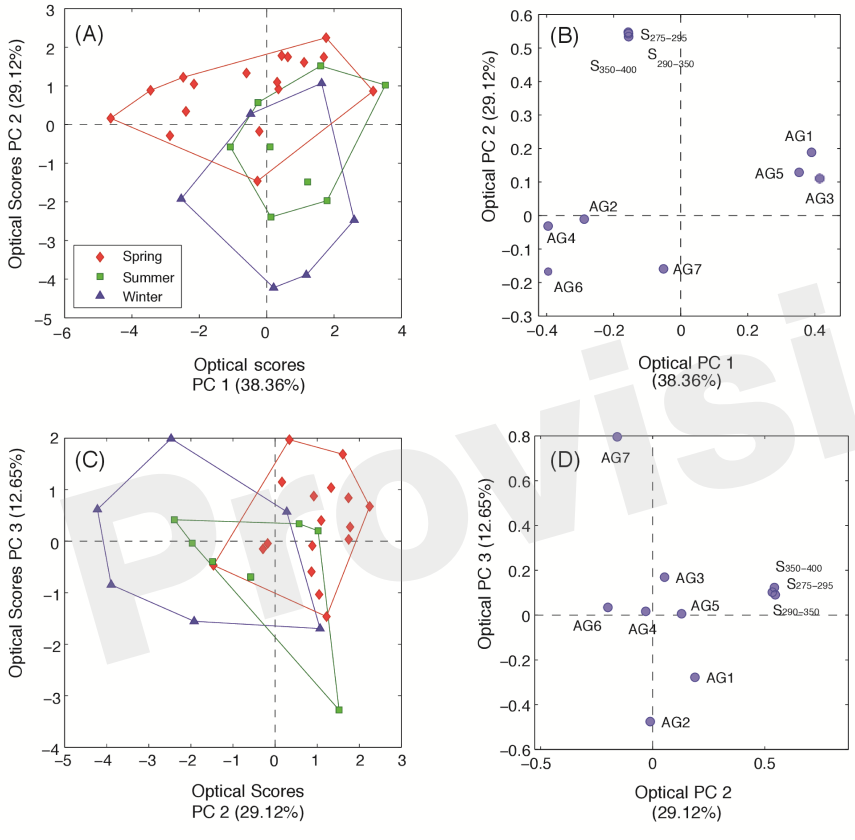

Figure 5.TIF

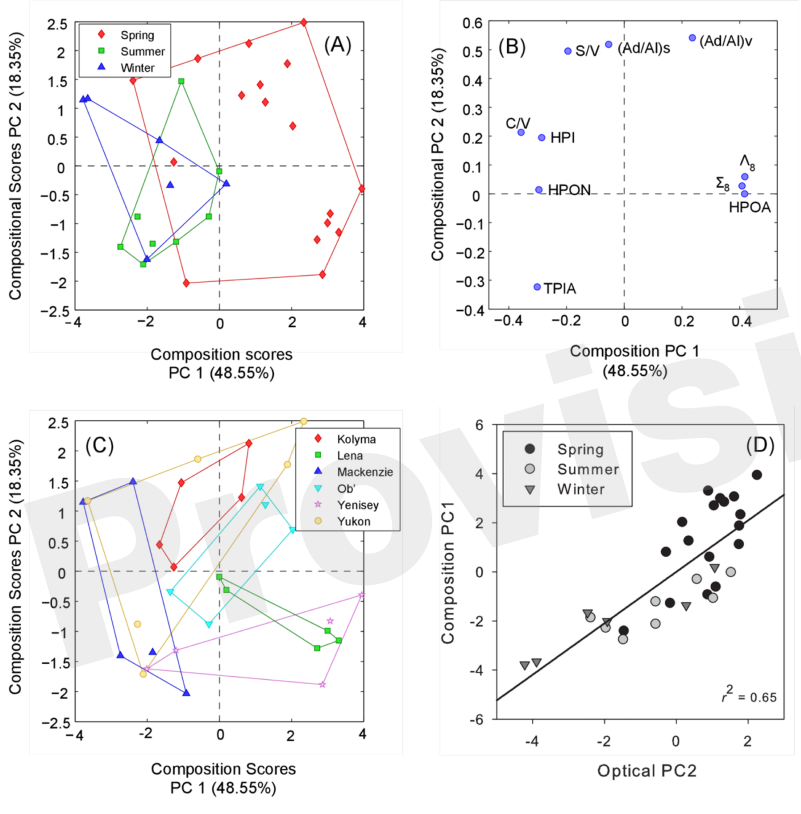

Figure 6.TIF